

Czech University of Life Sciences
Faculty of Agrobiolgy, Food and Natural Resources
Department of Plant Protection



Control of Cercospora leaf spot on sugar beet in the Czech Republic



Doctoral dissertation thesis

Author: Ram Kumar

BSc, Amity University, 2016

MSc, Chaudhary Charan Singh University, 2018

Supervisor: doc. Ing. Miloslav Zouhar, Ph.D.

Co- Supervisor: Ing. Marie Maňasová, Ph.D.

Prague, 2023

DEDICATION

This work is dedicated to my
Dear Mother, RAMA BAI
Dear Father, GAJENDRA SINGH
Sweet Wife, VISHAKHA

Statement of authorship

I hereby declare that I have written my dissertation thesis entitled “**Control of Cercospora leaf spot on sugar beet in the Czech Republic**” independently and on my own. All literature sources used in this thesis are properly cited according to requirements of the Faculty of Agrobiology, Food and Natural Resources, CULS Prague, and are listed in the chapter References and vice versa. Moreover, it is also to be declared that the research work presented here is original and has not been submitted to other institutions for any degree or diploma.

ACKNOWLEDGEMENTS

I would like to express my sincere gratitude to my supervisor asoc. Miloslav Zouhar and co-supervisor Dr. Marie Maňasová, for giving me the opportunity to pursue this doctoral program, valuable supervision and guidance throughout my doctoral program as well as independence to choose my work, kindness and relentless encouragement, and teaching me how to become a plant pathologist. My special thanks to our department head, prof. Ing. Pavel Ryšánek, CSc., for his constant encouragement and motivation. Special thanks to Dr. Jana Mazáková for teaching phytopathological techniques, which helped me a lot.

I would like to thank all the people who helped me in the completion of this state doctoral exam thesis. I owe special thanks to my family for their love and affection for me during my stay at CZU. I thank all my friends, especially Madhab Kumar Sen, Asad Ali, and Pratap Madhvadiya, for their help, for sharing knowledge, and the memorable times we had together.

I am very thankful to my family members, father, mother, wife, sister and sister-in-law for their unconditional love and support during my time away from home. My wife deserves special thanks for her love and staying with me all the stage of this doctoral program. If I can thank only one person, it will be my father.

TABLE OF CONTENTS

ACKNOWLEDGEMENTS	2
Chapter: 1 Introduction and objectives	6
1.1 Introduction	6
1.2 Objectives	7
1.3 Hypotheses.....	7
Chapter: 2 Review of literature	7
2.1 History of sugar production	7
2.2 Sugar beet-producing countries.	8
2.3 Sugar beet diseases	10
2.3.1 Cercospora leaf spot (CLS) disease.....	10
2.3.2 CLS disease symptom	10
2.3.3 Phanomyces root rot of sugar beet.....	11
2.3.4 Rhizoctonia root and crown rot.....	11
2.3.5 Beet necrotic yellow vein virus (BNYVV)	12
2.3.6 Importance of CLS Disease	12
2.4 Host rang and taxonomy of <i>Cercospora beticola</i>	12
2.4.1 Taxonomy	12
2.4.2 Host range, life cycle, and etiology	14
2.5 Fungicide resistance in <i>Cercospora beticola</i>	15
2.5.1 Target-site alterations	16
2.5.2 Target-site overexpression.....	16
2.5.3 Altered efflux pump activity.....	17
2.6 Management of Cercospora leaf spot	17
2.6.1 Resistance cultivars	17
2.6.2 Fungicides application.....	18
2.6.3 Biological control Agent (BCA)	18
Chapter: 3 Material and methods	20
3.1 Sample collection	20
3.2 Fungicide sensitivity assay	20
3.3 Artificial inoculation.....	20
3.4 Cloning of the partial <i>CbCyp51</i> gene from <i>C. beticola</i>	21
3.5 Three-dimensional structural validation and visualisation	22
3.6 Molecular docking and simulation studies	22

3.7 MD trajectories analysis	23
3.8 <i>C. beticola</i> <i>CbCyp51</i> gene copy number variation and expression analysis	23
3.9 RNA extraction, RNAseq library preparation and Illumina sequencing	26
3.10 RNAseq Analysis of resistant and sensitive isolates	26
3.11 Identification of Ergosterol Biosynthesis Genes	27
Chapter: 4 Results	28
4.1 Sample collection and fungicide sensitivity	28
4.2 Artificial inoculation.....	33
4.3 <i>Cercospora beticola</i> <i>CbCyp51</i> gene mutations	33
4.4 <i>C. beticola</i> <i>CbCyp51</i> gene copy number variation and expression analysis	34
4.5 <i>Cercospora beticola</i> <i>CbCyp51</i> protein structure validation	37
4.6 Impact of the Y464S mutation on propiconazole binding.....	41
4.6.1 Molecular docking studies	41
4.6.2 Behavioural dynamics of the wild-type and mutant-type systems.....	43
4.7 Impact of the Y464S mutation on prochloraz binding	45
4.7.1 Molecular docking studies	45
4.7.2 Behavioural dynamics of the wild-type and mutant systems.....	46
4.8 Impact of the Y464S mutation on epoxiconazole binding	48
4.8.1 Molecular docking studies	48
4.8.2 Behavioural dynamics of the wild-type and mutant-type systems.....	50
4.9 RNAseq study analysis.....	51
4.9.1 Selection of isolates of <i>C. beticola</i> for RNAseq study after exposure to epoxiconazole.....	51
4.9.2 Quality evaluation of RNAseq Alignments.....	52
4.9.3 Differentially Expressed Genes in epoxiconazole treated and untreated isolates	53
Chapter: 5 Discussion.....	57
5.1 Importance of CLS disease and its management.....	57
5.2 <i>CbCyp51</i> Gene Mutations in <i>C. beticola</i>	57
5.3 <i>CbCyp51</i> Gene Expression Analysis	58
5.4 Impact of the Mutations on Fungicide Binding.....	58
5.5 RNAseq study analysis.....	59
Chapter: 6 Conclusion	61
Chapter: 7 Publication	62
LIST OF ABBREVIATIONS	67
LITERATURE CITED	A

Chapter: 1 Introduction and objectives

1.1 Introduction

Sugar beet (*Beta vulgaris L.*) is one of the most economical crops grown in the Czech Republic and Europe's contribution is 45-50 of total world production. In the Czech Republic, in 2018 sugar beet harvested area was 64,70 thousand hectares and production was 3.72 million tonnes (world data atlas, 2018). The total crops losses reported due to plant disease are up to 25% of worldwide crop production per annum (Lugtenberg *et al.*, 2016). The diseases of sugar beet are one of the foremost constraints in the profitability in the cultivation of sugar beet around the world. *Cercospora* leaf spot (CLS) is one of the most economical important foliar disease of sugar beet, it can reduce yield and sugar quality up to 50% if unmanaged (Shane & Teng, 1992; Rossi *et al.*, 2000) . *Cercospora beticola* was first report by Saccardo in 1886, and after a short period, the CLS disease was reported as a severe issue in Europe and the United States. *Cercospora spp.* resistance was developed in the United States and Italy in the early 19th century(Stevanato *et al.*, 2014). CLS disease primarily infects sugar beet in warm and humid growing region. CLS symptoms usually appear after close crop canopy, especially on older leaves close to the soil. *Cercospora* leaf spots are visible and circular, about 3-4 mm in diameter with dark brown to reddish-purple. As the disease progresses, leaf lesions merge, and whole leaves die, which remain attached to the plant and later buried in soil, infecting sugar beet plant in the next cropping season.

Currently, fungicide applications with biological and resistant cultivars are using CLS management strategy to manage under field conditions. As of now, most sugar beet; cultivars are susceptible to the pathogen. CLS disease is primarily managed by several groups of fungicides recommended by Fungicide Resistance Action Committee (FRAC). However, the last decade's research revealed fungicide resistance from every group of fungicides, e.g. Quinone outside Inhibitors (QoIs), DeMethylation Inhibitors (DMIs) and Succinate dehydrogenase inhibitors (SDHIs) (Robbertse *et al.*, 2001; Bolton *et al.*, 2011; Rosenzweig *et al.*, 2019).

1.2 Objectives

1. To identify the region infected with CLS disease of sugar beet in the Czech Republic.
2. To isolate *Cercospora beticola* from sugar beet leaves in the Czech Republic from sugar beet fields.
3. To perform artificial inoculation of *Cercospora beticola* on sugar beet plants under in-vitro conditions.
4. To study fungicide sensitivity of *Cercospora beticola* in-vitro condition.
5. To assess the presence of fungicide resistance in *Cercospora beticola* populations in the Czech Republic.

1.3 Hypotheses

1. The cultivated sugar beet (*Beta vulgaris L.*) varieties in the Czech Republic are highly infected by *Cercospora beticola*.
2. The isolated *C. beticola* strains are resistant against different DMI fungicides.
3. Mutations within the coding region of *CBCYP51* and overexpression of *CBCYP51* gene might be responsible for Resistance against DMI fungicides in *C. beticola*.
4. Gene amplification might also result in gene overexpression.

Chapter: 2 Review of literature

2.1 History of sugar production

Sugar can be categorised into three groups: monosaccharides (fructose, glucose, galactose, and ribose), disaccharides (sucrose, lactose, and maltose), and polysaccharides (starch, glycogen, and cellulose). Sucrose is a disaccharide, which is comprised of two monosaccharides (glucose and fructose). Sucrose is the most common sugar that humans consume, and sugar is commonly described as sucrose (Richardson, 2010).

Sucrose is mainly extracted from two crops: sugarcane (*Saccharum officinarum L.*) and sugar beet (*Beta vulgaris L.*). Sugar cane has been cultivated worldwide since 1000 BC in tropical and subtropical regions. The sugarcane contribution to sucrose's total production accounts for 80% and 20% of sugar beet contributes to sugar production worldwide (FAO, 2014). The top five sugarcane producers are Brazil, India, China, Thailand, and Pakistan (FAO, 2015). Comparison of sugar beet with sugarcane is a relatively old source of sucrose in tropical and subtropical regions. On the other hand, sugar beet is temperate region crop relatively new sucrose source, which has been cultivated since the 17th century (Richardson, 2010). In 2018, France was a major sugar beet producer by the United States, Russia, Germany, and Ukraine in Figure 1 (FAO, 2018).

The ancestor of sugar beet is the wild sea beet (*B. vulgaris ssp. Maritima*) grown on the coasts area of the United Kingdom, mainland Europe, and North Africa. In the earlier time, people considered beets as vegetables and kitchen garden plants. In the 17th century, beets were cultivated as a field crop and used as cattle food in France and German (Francis, 2006). The modern-day sugar beet industry's foundation was laid by the German chemist Andreas Margraff in 1747. However, the public did not accept his discovery. After forty years, Franz Carl Achard Marggraf, one of the students recognised as the 'Father of the beet sugar industry', developed the industrial procedure of extracting sugar from White Silesian beets and built the first beet sugar factory in 1801 at Kunern in Lower Silesia. The White Silesian beets, bred and harvested by Achard himself, were described as white skin and flesh and having a conical shape with the exceptional characteristic of high sucrose concentration. The sugar beet industry grew during the Napoleonic Wars (Richardson, 2010).

Since sugarcane produced in France's tropical colonies could not be conveyed to France because Great Britain disconnected all the imports to France, Napoleon provided financial assistance to promote France's local sugar beet industry from 1811-13. Unfortunately, the sugar beet industry was not succeeding well with the fall of Napoleon's empire. The second development of the beet sugar industry promoted sugar extraction techniques and the government's policy for sucrose (Francis, 2006).

2.2 Sugar beet-producing countries.

In 2018, 275.49 million tons of sugar beet were produced worldwide in Figure 1 (FAOSTAT Dec. 20, 2020). The Czech Republic produced 3.72 million tons which are 1.35% of the world's sugar beet production (<https://knoema.com/ATLAS>, 2018). In 2018, the European Union was the world's largest sugar beet producer, producing 184.72 million tons Figure 3 (FAO, 2018).

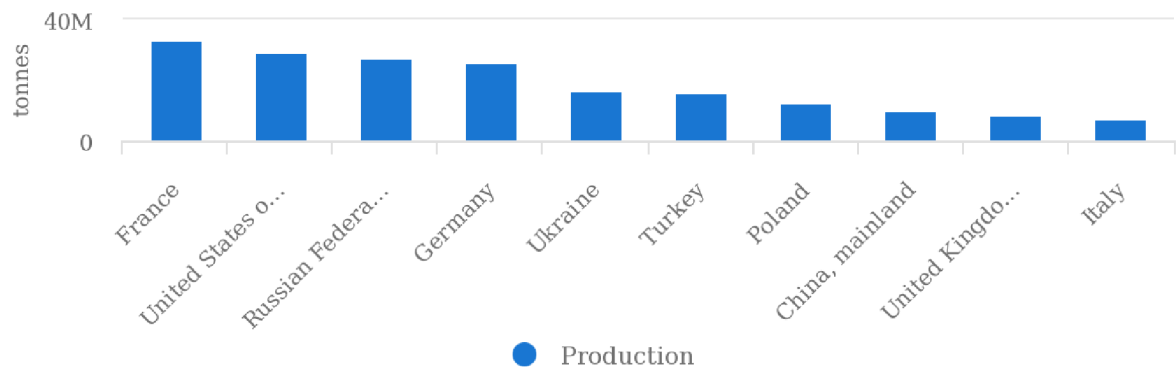


Figure 1 The top 10 sugar beet-producing countries from 1994-2018 (FAO 2018).

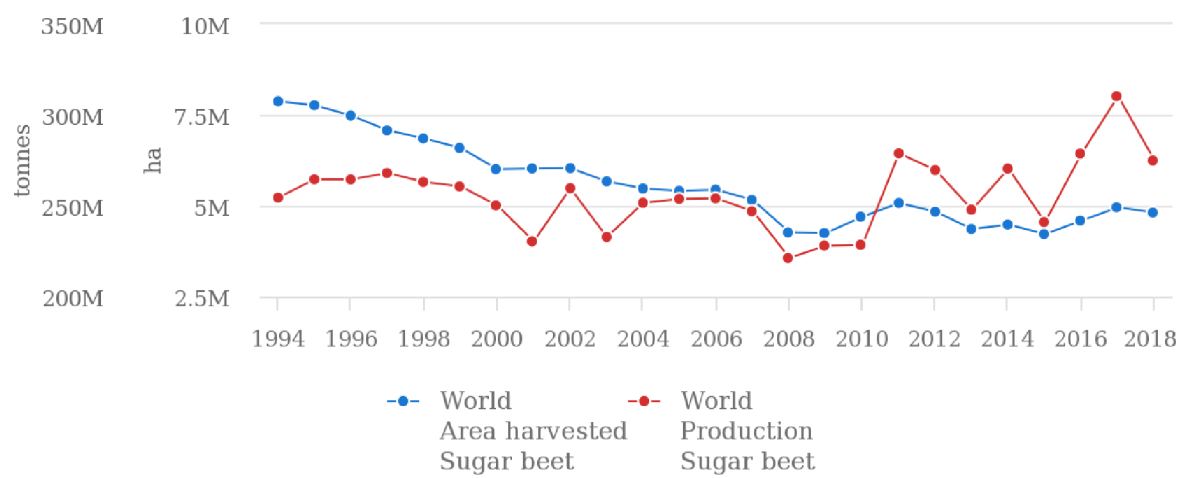


Figure 2 Production /Yield quantities of sugar beet around the globe since 1994-2018 (FAO, 2018)

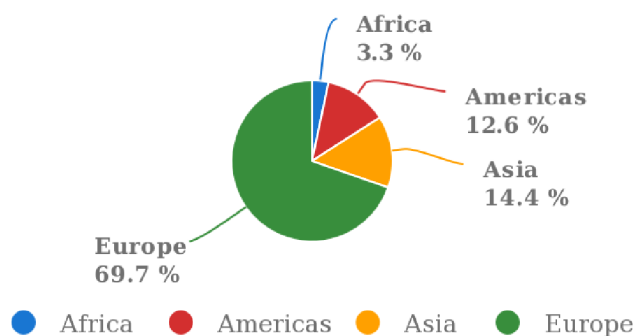


Figure 3 The sugar beet production in each continent from 1995-2018 (FAO, 2018).

2.3 Sugar beet diseases

Biotic agents can cause diseases (plant pathogens) such as fungi, bacteria, nematodes, viruses, oomycetes, arthropods, and parasitic plants in the sugar beet. Plant pathogens can significantly reduce the quality and yield of sugar beet. In the Czech Republic, most common sugar beet diseases are *Cercospora* leaf spot (CLS), *Fusarium* yellows, Rhizomania, *Aphanomyces* root rot, *Rhizoctonia* crown root rot, and *Fusarium* yellowing decline (Řezbová *et al.*, 2013).

2.3.1 *Cercospora* leaf spot (CLS) disease.

Cercospora leaf spot disease is the most economical foliar disease of sugar beet caused by *Cercospora beticola* (Sacc. 1876) (Hill, Jacobsen, & Panella, 2009; Skaracis, Pavli, & Biancardi, 2010). Saccardo, P. A. in 1876, first reported CLS (Chupp, 1953). *Cercospora beticola* can develop over wintertime as stromata in infected sugar beet leaf residue on or directly beneath the soil surface (Khan *et al.*, 2008). Sporulation can occur from over-wintered stromata, and the resulting conidia are produced on sugar beet leaf surfaces predominantly by wind and water splash. *Cercospora beticola* penetrates stomata to enter the apoplast (Steinkamp *et al.*, 1979), where effectors are generated by the invading hyphae that facilitate disease formation. Conidia are produced in necrotic leaf spots and can be spread by wind and water splash to start another disease cycle. Characteristic symptoms are circular spots with a grey centre and red-purple margins on a 3-4 mm leaf. Combining in later phase into large circular leaf spot leads to the reduction of photosynthetic activity of these leaves, which cause result in less fixed carbon, cause reduced root and extractable sucrose yields. The losses in recoverable sucrose as high as 30% are widespread under heavy disease conditions, and revenue losses as high as 43% (Wolf *et al.*, 1998; Wolf & Verreet, 2002, 2009).

2.3.2 CLS disease symptom

Cercospora leaf spot symptoms first appear as individual, round spots that are tan to light brown with reddish-purple borders. As the disease progresses, each spot coalesce. Heavily infected leaves first become yellow and, in the end, turn dark-brown and necrotic. Blighted leaves soon collapse and fall to the ground but remain attached to the crown. Healthy leaves are usually less severely affected and remain green by CLS (Rangel *et al.*, 2020a).



Figure 4 Symptoms of *C. beticola* leaf spot on a leaf of sugar beet field in leaf in the left side and CLS infected sugar beet field on the right side.

2.3.3 Phanomyces root rot of sugar beet

Chronic root rot and damping off of sugar beet caused by *Aphanomyces cochlioides* Drechs. is a major constraint in cultivation of sugar beet worldwide. The disease is responsible for reductions in plant numbers, yield and sugar yield (Windels, 2000; Harveson *et al.*, 2002). Sugar yield can be reduced by as much as up to 30% worldwide (L. Persson and Å. Olsson, unpublished data) in highly diseased fields. *Aphanomyces cochlioides* can be found in majority of soil and these fields have a medium to high risk of *Aphanomyces* root rot. In Minnesota and North Dakota in the USA, more than half of the acres planted with sugar beet are infested with *A. cochlioides* (Windels *et al.*, 2007). Disease progression is favoured by high temperatures and wet soils (Windels, 2000). Frequent cultivation of host crops, such as sugar beet, spinach and table beet, increases inoculum density in the soil (Papavizas, 1974). *A. cochlioides* has problems with diseases have been reported worldwide from a number of countries in Europe, e.g. Netherlands, Belgium, Germany and Poland (Van Swaaij *et al.*, 2001; Büttner *et al.*, 2003; Piszczek, 2004) as well as from the USA (Harveson *et al.*, 2002).

2.3.4 Rhizoctonia root and crown rot

Rhizoctonia root is an economically important disease of sugar beet worldwide. It is caused by the soil-borne fungal pathogen *Rhizoctonia solani* KUHN, up to 10% of the total European and United States sugarbeet area is infected by the disease (Herr, 1996; Büttner *et al.*, 2003). In *Rhizoctonia* infected fields, yield and sugar content are reduced by 50%. Sugar beet storing and

quality are affected, resulting in difficulties while processing beet in the sugar factory (Herr, 1970; Herr, 1996).

2.3.5 Beet necrotic yellow vein virus (BNYVV)

BNYVV is a portion of the genus *Benyvirus* within the family Benyviridae (Gilmer *et al.*, 2017). The virus is the causal agent of rhizomania disease in sugar beet, and is distributed worldwide (McGrann *et al.*, 2009) and causes a dramatic decrease in sugar beet yield and sugar content. BNYVV disease symptoms are including wineglass like shape, reduced size, and necrosis of vascular tissue can be observed on diseased taproots. Extensive proliferation of lateral roots (LRs) leads to a root beard, a feature of the rhizomania disease. Systemic symptoms on leaves are categorised by vein necrosis and yellowing but can be seldomly found in the field. The virus is spread by the soil-borne plasmodiophoromycete *Polymyxa betae* that infects the root soft tissue of sugar beet plants (Tamada & Kondo, 2013).

2.3.6 Importance of CLS Disease

The most common and devastating foliar disease of sugar beet worldwide is CLS (Holtschulte, 2000). The disease was first reported on *Beta cicla* in Italy by Saccardo (1876) but now has been recognised across the globe wherever sugar beet is cultivated. CLS is most destructive in warm, humid growing areas (Majumdar *et al.*, 2020). The main adversity is the loss of sucrose, reaching up to 50% under uncontrolled medium to high disease stress (Rangel *et al.*, 2020a). Further yield losses occur as a result of increased impurities that convolute sucrose recovery processes, which result in higher processing costs and decreased extractable sucrose (Shane & Teng, 1992). Large economic losses were reported in sugar beet crops in southern Germany in the late 1980s and early 1990s due to extreme CLS epidemics (Wolf & Verreet, 2005). In the USA, Minnesota and North Dakota reported losses from CLS in 1998 approx at \$113 million from yield decrease and fungicide application costs (Secor *et al.*, 2010).

2.4 Host rang and taxonomy of *Cercospora beticola*

2.4.1 Taxonomy

The pathogen *C. beticola* is an imperfect filamentous fungus with no known sexual stage (Weiland & Koch, 2004). This often could confirm erroneous as leaf spot diseases caused by some species of *Cercospora* have been described on weeds in the presence of and on crop species in variation with leaf and root crops such as sugar beet (Rangel *et al.*, 2020b). Although specific host range studies with *C. beticola* have been reported, systematic investigation

confirming the host range of mycosphaerellaceae (Cercosporoid) fungi isolated from the leaf spots of sugar beet, an essential characteristic in *Cercospora* taxonomy, hasn't to our knowledge been described. Production by *C. beticola* and related species of the plant toxins cercosporin has been a valuable taxonomic tool in a broad sense. Still, it is too inconstant in its expression in culture between *Cercospora* species strains and different culture media preparations to be relied on for slight taxonomic separation (Goodwin *et al.*, 2001).

Table 1 Taxonomy of *Cercospora beticola* in ascending order

Species	<i>Beticola</i>
Genus	<i>Cercospora</i>
Family	Mycosphaerellaceae
Order	Capnodiales
Class	Dothideomycetes
Phylum	Ascomycota
Kingdom	Fungi

None of the *Cercospora* species included in the monophyletic with *C. beticola* based on ribosomal DNA (rDNA) sequences possesses a known teleomorph, proposing that this function may have been lost throughout the evolution of the group (Goodwin *et al.*, 2001). Nevertheless, hyphal inosculation or an elusive mating system may encourage genome exchange in *C. beticola*, supporting genetic diversity within populations. Surveys are revealing diversity in fungicide resistance in *C. beticola* under fungicide pressure (Karaoglanidis *et al.*, 2000). Analysis by amplified fragment length polymorphism (AFLP) compression of single-spore isolate of *C. beticola* in two independent experiments in Europe and the USA shows substantial genetic variation in natural populations (Weiland & Halloin, 2001).

This apparent genome agility in *C. beticola* combined with limited sequence variety in rDNA regions of related *Cercospora* species provides confusion in the genus's taxonomy (Goodwin *et al.*, 2001). Although both development morphology in culture and virulence have been used as characters for the grouping of *C. beticola* isolates (Chupp, 1953), use of this information in the description of distinctive field strains has not gained acceptance (Chupp, 1953).

2.4.2 Host range, life cycle, and etiology

Cercospora beticola has been causing symptoms in all members of beta wherever they were tested. *C. beticola* infects plant species of the genus *Beta* and a few species in the Chenopodiaceae, as well as members of the genera *Spinacea*, *Atriplex*, and *Amaranthus* has been noted that leaf spot-causing fungi on weed species having needle-shaped. However, many other family members, such as Chenopodiaceae, had shown leaf spot symptoms when they were inoculated with the pathogen. Reports of CLS disease on non-beta plant species attributed to *C. beticola* lack evidence across pathogen isolation and inoculation to *B. vulgaris* (Chupp *et al.*, 1953). Sugar beet plant naturally infects when stroma in infected leaf debris. It is hypothesised that sporulation might arise directly from over-wintered stroma in organic matter or it may be anticipated by saprophytic, vegetative growth of *C. beticola* mycelia. In favourable condition, infection commenced, water splash, wind, and insects work as a vector to disperse spores primarily on the leaf surface of sugar beet plants, demonstrating *C. beticola* life cycle Figure 5 (Rangel *et al.*, 2020b). *Cercospora beticola* septate conidia deposited on host plant, petiole surfaces germinated under high humidity circumstances (up to 95 per cent), leaf wetness, and growth in the direction of stomata's throughout the before-infection stage (Kaiser & Varrelmann, 2009).

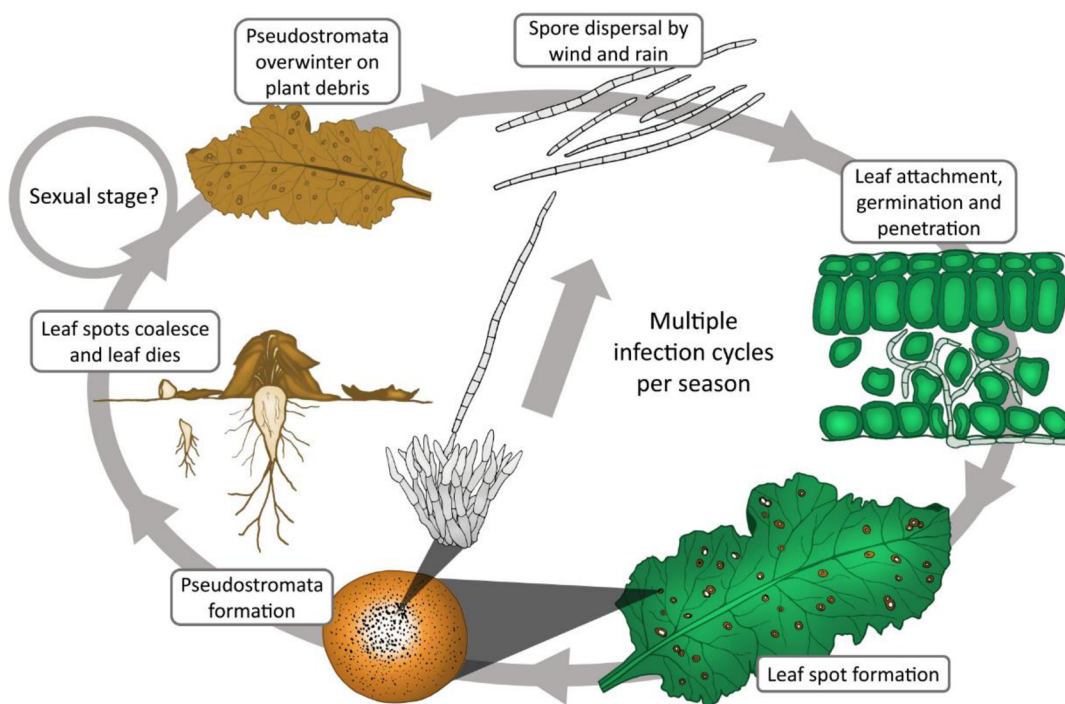


Figure 5 *Cercospora* leaf spot (CLS) disease cycle in sugar beet. Disease infection is initiated by airborne or splash dispersed conidia that permeate the sugar beet leaf via stomata and provide growth to intercellular hyphal development. CLS spot form on the leaves after the switch to necrotrophy, which develops symptoms within 7 days. Pseudostromata developed in the lesion, and *C. beticola* asexually produce spores, leading to multiple infection cycles in one growing season. The Pseudostromata can also survive to overwinter in plant debris at the end of the season (Image source)(Rangel et al., 2020b).

2.5 Fungicide resistance in *Cercospora beticola*

Fungicides have been used for over two centuries to protect plants against pathogenic fungi and due to over reliance on fungicides, it become new problem in plant disease control. The ‘fungicide resistance’ considering is a different phenomenon, sometimes called ‘acquired resistance’. Eventually, during the years of commercial use of a fungicide, populations of the target pathogen can rise that is no longer sensitive to be controlled effectively (Brent & Hollomon, 1995).

Fungicide resistance is a constant, inheritable alteration by a fungus to a fungicide, resulting in reduced sensitivity of the fungus towards the fungicide. Resistance may result from multiple or single nucleotide polymorphisms. Resistant strains typically arise from a very low

natural rate of genetic mutation, and these strains are less affected by the fungicide application rate. Since the fungicide can effectively control sensitive strains, resistant strains may become dominant in fungal pathogen populations under selection pressure of fungicide use over time, therefore, disease control failures may eventually occur (Dekker, 1982).

Fungicide resistance can be categorised into two basic mechanisms: target-site based and nontarget-site-based resistance. Target-site-based resistance mainly requires single or multiple nucleotide polymorphisms, increased target gene amplification, and target gene overexpression (Ma *et al.*, 2006; Bolton *et al.*, 2013; Muellender *et al.*, 2021). These mechanisms reduce the fungicide's ability to inhibit the target enzyme. Nontarget site-based resistance decreases the concentration of active fungicide related to the target site protein by reducing translocation and vacuolar sequestration, enhancing metabolism and/or reducing absorption. Moreover, more than one mechanism might associate resistance within a species, a population, and a single individual (Sen *et al.*, 2021). Hence, the exact resistance mechanisms must be revealed before they become a significant issue worldwide (Muellender *et al.*, 2021).

2.5.1 Target-site alterations

Point mutations in *C.beticola* in target (CYTB) site that encode an amino acid change from phenylalanine to leucine at location 129 (F129L), glycine to arginine at location 137 (G137R) or glycine to alanine at location 143(G143A) have been associated with resistance to quinone outside inhibitors (QoI) fungicides (Fisher N 2008). Point mutation in *CbCyp51*, associated with Resistance in DeMethylation Inhibitors (DMIs), has been reported in *C. beticola* Y464S, L144F and I309T linked with L144F were found to be associated with reduced sensitivity (Muellender *et al.*, 2021). Furthermore, mutations I387M, M145W and E460Q with M145W were found (Muellender *et al.*, 2021).

2.5.2 Target-site overexpression

The *CbCyp51* gene was isolated and a study of transcriptional levels of the *CbCyp51* gene showed that over-expression was strongly associated with the highly DMIs resistant phenotype. Afterwards, Karaoglanidis and Thanassouloupoulos (2002) tested phenotypic stability of resistance to flutriafol with strains of *C. beticola*. After successive transfers of isolates either in vitro or in vivo in the absence of flutriafol, sensitivity was unchanged. Over-expression of the target protein results in a general decrease in sensitivity towards DMIs (Ma *et al.*, 2006).

2.5.3 Altered efflux pump activity

The active excretion of the fungicide by over-expressed ATP-binding cassette (ABC) transporters was described as responsible for a loss of efficacy towards DMIs in field populations of *Penicillium digitatum* *Zymoseptoria tritici*, or *Botrytis cinerea*. The fungicide might affect the target protein, but the active excretion of the fungicide separates the fungicide from the target protein (Rossi *et al.*, 2000; Bolton *et al.*, 2016).

2.6 Management of Cercospora leaf spot

In early 19th century, inorganic copper was used by farmers to manage *C.beticola* in sugar beet fields (Weiland & Koch, 2004). Not until over 50 years later was a systematic effort to develop broad-spectrum chemistry fungicides. These efforts have significantly advanced sugar beet cultivation and increased yield and sugar quality affected by the CLS disease. Both synthetic and natural derived fungicides, systemic and protectant are used to manage *C. beticola* in sugar beet (Karaoglanidis *et al.*, 2000). However, not all available fungicide chemistries can be used because of environmental health considerations (Weiland & Koch, 2004).

Since CLS multicycle disease, up to four fungicide applications are needed for one growing period (Secor *et al.*, 2010). Most of the fungicides that apply to manage *C. beticola* pathogen in sugar beet belong to the DMIs, MBCs, (QoIs), and (SDHIs). Cultivation of sugar beet has become more profitable because of the convenience of using different fungicides, e.g. DMIs, MBCs, and QoIs (Karaoglanidis *et al.*, 2000). According to Fungicide Resistance Action Committee (FRAC), these groups were categorised as medium risk. Despite the effectiveness of fungicides, the lack of effective pest management plans and overreliance on selected groups has led to the evolution of fungicide resistance in *C. beticola* populations worldwide (Nikou *et al.*, 2009; Rosenzweig *et al.*, 2019). Recently, the development of fungicide resistance has been an alarming issue in plant disease control. It leads to finding alternative methods like an integrated disease management approach, which will reduce fungicide resistance in *C. beticola* (Dekker, 1982).

2.6.1 Resistance cultivars

Cercospora leaf spot disease resistance to sugar beet cultivars is easily available in the Czech Republic and other countries where *C. beticola* infection frequently occurs (Mechelke, 2000). The sugar beet cultivars conferred partial resistance, but full potential is seen under severe infection; under epidemics, sugar quality and yield are considerably increased in resistant cultivars than in susceptible ones if fungicide was not used (Rossi *et al.*, 1999). However, in severe infection cases, host resistance is not enough to manage disease infection, and yield

losses occur (Rossi *et al.*, 2000). In resistance cultivars, fungicide application always does not significantly improve crop production compared to the susceptible cultivars (Rossi *et al.*, 1999). However, high-yielding cultivars treated with fungicide application are favourable over resistant varieties, which remain to exhibit reduced yield compared with high-yielding varieties if no infection occurs (Rossi *et al.*, 1999). It has been reported that resistant cultivars yield lower if no disease infection occurs than susceptible cultivars (Miller *et al.*, 1994; Ossenkop *et al.*, 2002).

2.6.2 Fungicides application

The planning of sustainable management programme for CLS disease in the Czech Republic and other countries based on rotation of different fungicides, e.g. DMIs, MBCs, SDHIs and QoIs, which are registered in different countries for CLS disease management. DMIs group of fungicides e.g. propiconazole, prochloraz and epoxiconazole, are demethylation inhibitor that interferes sterol 14 alpha-demethylase activity and C14- demethylation step during sterol development (Robbertse *et al.*, 2001). Resistance in *C. beticola* to DMIs is also widespread in sugar beet across Europe (Karaoglanidis *et al.*, 2003; Karaoglanidis & Bardas, 2006). Moderate CLS disease control has been reported from the SDHIs group alone or in combination with other FRAC groups (Vaghefi *et al.*, 2017). SDHIs fungicides work on ubiquinone binding sites within the mitochondrial succinate dehydrogenase principal to respiration inhibition from FRAC group 7 (Sierotzki & Scalliet, 2013). The current recommendation for CLS management is to apply the first fungicide spray on an average one CLS lesion per leaf, with subsequent applications repeated based on level of infection or, in some cases, the reapplication recommendations of specific products from the manufacturer company according to FRAC group.

2.6.3 Biological control agent (BCA)

Plant diseases are primarily managed by synthetic chemicals, widely available worldwide, and these fungicides significantly increase the cost of cultivation. However, the frequently used of pesticides has caused some serious environmental issues. Biological disease control (BCA) using antagonists is an environmentally sustainable alternative to synthetic fungicides. The most promising microorganisms for sustainable crop disease management are, e.g. *Bacillus spp.*, *Coniothyrium minitans*, *Gliocladium catenulatum*, *Pseudozyma flocculosa*, *Trichoderma spp.* and *Pythium oligandrum*. BCA's main characteristic is that they are very specific for a plant pathogen, considered harmless to nontarget microorganism, and beneficial for biodiversity. The level of disease management is achieved by applying BCAs on plants close

to or equivalent to the application of fungicide. Application of a fungicide in apple collar rot disease controlled up to 100% infection, whereas applying BCAs disease control levels between 79% – 98% (Alexander & Stewart, 2001). A *Bacillus amyloliquefaciens* BCA controls up to 77% disease infection of *P. digitatum* in mandarin fruit compares with 96% fungicide enilconazole (Hao *et al.*, 2011) Table 2. Several studies have confirmed that biocontrol can also be used effectively against postharvest diseases.

Table 2 Biological control agent for plant diseases

Pathogen	Disease control agent	Inhibition	Reference
<i>Phytophthora cactorum</i>	<i>Flavobacterium</i>	79%	Alexander & Stewart, 2001
<i>Phytophthora cactorum</i>	<i>Oidiodendron</i>	85%	Alexander & Stewart, 2001
<i>Phytophthora cactorum</i>	<i>Microsphaeropsis</i>	98%	Alexander & Stewart, 2001
<i>Phytophthora cactorum</i>	<i>Trichoderma harzianum</i>	89%	Alexander & Stewart, 2001
<i>Phytophthora cactorum</i>	<i>Trichoderma koningii</i>	93%	Alexander & Stewart, 2001
<i>Phytophthora cactorum</i>	<i>Paecilomyces</i>	93%	Alexander & Stewart, 2001
<i>Phytophthora cactorum</i>	<i>Metalaxyl + Mancozeb</i>	100%	Alexander & Stewart, 2001
<i>Pseudocercospora musae</i>	<i>Bacillus subtilis</i> B106	72%	Fu et al., 2010
<i>Pseudocercospora musae</i>	<i>Bacillus subtilis</i> B106	48%	Fu et al., 2010
<i>Plasmodiophora brassica</i>	<i>B subtilis</i>	>80%	Peng et al., 2011
<i>Plasmodiophora brassica</i>	<i>Gliocladium catenulatum</i>	>80%	Peng et al., 2011
<i>Phytophthora meadii</i>	<i>Alcaligenes sp. EIL-2</i>	63%	Abraham et al. 2013
<i>Phytophthora meadii</i>	<i>Alcaligenes sp. EIL-2</i>	30%	Abraham et al. 2013
<i>Penicillium digitatum</i>	<i>B. amyloliquefaciens</i> HF-01	77%	Hao et al., 2011
<i>Penicillium digitatum</i>	<i>Imazalil</i>	96%	Hao et al., 2011
<i>Phytophthora capsici</i>	single bacterium	32–73%	Kim et al., 2008
<i>Phytophthora capsici</i>	mix of 3 bacteria	99%	Kim et al., 2008
<i>Phytophthora capsici</i>	<i>B. subtilis</i> R33	87%	Lee et al., 2008
<i>Phytophthora capsici</i>	<i>B. subtilis</i> R13	71%	Lee et al., 2008
<i>Fusarium sambucinum</i>	<i>Serratia plymuthica</i> 5–6	75%	Gould et al., 2008
<i>S. subterranea</i>	<i>Aspergillus versicolor</i> Im6–50	70%	Nakayama et al. 2013
<i>S. subterranea</i>	<i>Aspergillus versicolor</i> Im6–50 + fluazinam	93%	Nakayama et al. 2013
<i>B. cinerea</i> LU829	<i>Trichoderma atroviridae</i> LU132	77%	Gardiner et al., 2009
<i>B. cinerea</i> LU829	<i>Trichoderma atroviridae</i> LU132	88%	Gardiner et al., 2009
<i>B. cinerea</i> LU829	<i>Fenhexamide</i>	71%	Gardiner et al., 2009
<i>B. cinerea</i> LU829	<i>Trichoderma atroviridae</i> LU132 + <i>Fenhexamide</i>	100%	Gardiner et al., 2009
<i>Ralstonia solanacearum</i>	<i>Phage PhiRSL1</i>	100%	Fujiwara et al., 2011

Chapter: 3 Material and methods

3.1 Sample collection

From 2018 to 2020, Collected leaves with CLS symptoms from infected sugar beet fields across the Czech Republic. To retain heterogeneity among the samples, we used different collection bags to store leaves samples from individual fields. Samples were handled in the laboratory of the Department of Plant Protection, Czech University of Life Sciences, Prague, Czech Republic, on the same day immediately after collection. Cut visible leaf spots from each leaf with a cork borer (20 mm). Later cutting, the individual leaf pieces were disinfected with 20% bleach and washed twice with distilled water to remove bleach and dried by blotting on sterile filter paper. Then, the leaf pieces from each leaf were further processed according to Krug (Krug, 2004). After two weeks, the petri plates were stored at 4 °C for future experiments.

3.2 Fungicide sensitivity assay

Two hundred fifty isolates were screened against three DMIs fungicides, propiconazole, prochloraz, and epoxiconazole. The active ingredients of each fungicide were obtained from Sigma-Aldrich, United States. The fungicides were suspended in dimethyl sulfoxide (DMSO) to prepare the stock solution of 0.10 mg ml⁻¹ and 10 mg ml⁻¹. Fungicide dose-response assays were conducted in PDA to obtain from HiMedia, India Petri plates with three replicates and serial 10-fold dilutions from 0.001 µg ml⁻¹ to 10 µg ml⁻¹. A control Petri plate containing PDA with DMSO was used as a control for comparison. After 14 days, radial growth inhibition was measured vertically and horizontally to be compared with untreated PDA plates, according to Wong and Wilcox, 2002. EC50 or 50% inhibitory effect values were analysed for all three fungicides utilising GraphPad Prism software (9.0.0) for Windows OS (GraphPad Software, San Diego, CA, US), based on the mean colony diameter and radial growth of each isolate. The resistance factor (RF) was calculated as the EC50 of the resistant isolates and the EC50 of the sensitive isolate. From the fungicide sensitivity assay, out of 250 total 20 highly sensitive and resistant isolates are screened, which is shown in (Table 4).

3.3 Artificial inoculation

Cercospora beticola biotype for artificial inoculation was isolated from CLS-infected leaves of sugar beet plant collected from the Czech Republic from 2018 to 2020. All the *C.beticola* biotypes were maintained at 4 °C on PDA. *C.beticola* biotypes were scraped and filtered through the 3 layers of sterile cheesecloth with double distilled water and spore suspension was collected in a falcon tube. The spore suspension was used for isolates spore production on clear V8 media (Tuite, 1969). The selected isolates from chemical sensitivity were grown for 10 days

of incubation under fluorescent light at 24 °C-26 °C on the clear V-8 media. After 10 days, spore colonies were rinsed with 15 ml distilled water and measuring the fitness component of spore suspension was adjusted to 8×10^3 spores per ml. before the inoculation all biotype suspension was added with on droplet of 0.1% Tween. For the artificial inoculation, 3 weeks old sugar beet plants were transferred to the greenhouse's growth chamber. The spore suspension was sprayed on sugar beet plants from each biotype, and 2 pots were sprayed from each isolate on susceptible and resistant cultivars. After potted inoculation plants were covered to maintain high humidity for 24 hours. The condition set in the growth chamber was 22 °C at night, 26 °C at night and relative humidity approx. 95% for 2-3 weeks. After 15 days, symptoms of CLS disease were cleared visible on sugar beet leaves.

3.4 Cloning of the partial *CbCyp51* gene from *C. beticola*

Mycelial samples from each resistance and sensitive isolate were grown in potato dextrose agar (PDB) for total genomic DNA (gDNA) extraction. Before the extraction, the mycelial samples were scratched from PDA plates and transferred to 250 ml flasks containing 50 ml of PDB (potato dextrose broth, HiMedia, India). The setup was kept on a shaker (set at 200 rpm) at 24°C-26°C for 96 hours. After 96 hours, the mycelial samples were filtered through cheesecloth and used for gDNA isolation. The GenElute™ Plant Genomic DNA Miniprep Kit (Sigma-Aldrich, US), following the manufacturer's instructions, was used to extract gDNA from the fungal isolates. *CbCyp51* gene-specific primers were designed in Primer 3 software based on the publicly available sequence of the *CbCyp51* gene from *C. beticola* (GenBank Acc. No. KU665583.1). The list of primers is defined in Table 3. PCR was performed using a C1000 thermocycler (Bio-Rad, Hercules, USA) with 30 ng of total gDNA per reaction. The thermocycler was programmed at an initial denaturation step at 95 °C for 5 min, followed by 35 cycles of 5 s at 95 °C, 10 s at 58 °C to 62 °C (based on the annealing temperature of the primer pair), and 2 min at 72 °C along-with a final extension step for 10 min at 72 °C. The PCR-amplified products were separated in a 1.5% agarose gel and subsequently purified using a MinElute Gel Extraction Kit (Qiagen, Hilden, Germany) following the manufacturer's instructions. After that, the amplicons were cloned using a CloneJET PCR Cloning Kit (Thermo Scientific, US) and transformed into DH10B competent cells (Thermo Scientific, US) according to the manufacturer's instructions. The positive clones were screened by colony PCR using insert-specific primers (pJET1.2 forward and reverse sequencing primers, provided along with CloneJET PCR Cloning Kit). Colony PCR was performed corresponding to the manufacturer's instructions provided along with the cloning kit. Following the positive clones

screening, plasmid DNA was isolated using an Ultraclean™ plasmid prep kit (Mo Bio, United States), according to the manufacturer's instructions and sent for custom DNA sequencing (Eurofins Genomics). The plasmid DNA integrity was assessed by running the samples on a 1% agarose gel before sending the samples for sequencing.

3.5 Three-dimensional structural validation and visualisation

SWISS-MODEL (<https://swissmodel.expasy.org/>) was used to predict the 3D structures of the wild-type (WT) *CbCyp51* and mutant-type (MT) *CbCyp51*. The best structure was chosen based on the QMEAN score function. The structures were further validated and assessed in the PROCHECK server (<https://servicesn.mbi.ucla.edu/PROCHECK/>) for the error value and the Ramachandran plot. Chimera 1.15rc visualised all the predicted 3D structures.

3.6 Molecular docking and simulation studies

In this study, we used PyRx 0.8 Autodock Vina module (grid box size 68.41 for x 61.57 for y and 64.51 for z-axis) was utilised to perform a series of protein-ligand docking studies to identify the most reliable binding pose and energy. Protein-ligand docking was visualised and analysed by Chimera 1.15cr at 1st, and then, more detailed analyses for interacting amino acids with the ligands were performed with IOVIA Discovery Studio Visualizer. Molecular dynamics simulations were completed at 300 K with the GROMACS 2020.1 package in the Ubuntu Linux system by utilising the OPLS-AA force field (protein system) and CHARMM36 (protein-ligand system) force-field. All systems were packed in a 10 Å dimension cubic water box using the gmx editconf module of boundary condition setup and solvation along with the gmx solvate module. Further, the simulation system was engrossed in a simulation box with a point charge SPC216 (protein only) and TIP3P (protein-ligand) water-model. Na⁺ and Cl⁻ ions were added to the system box for neutralisation of the simulation system, and the physiological system was maintained (0.15 M) using the gmx genion module. For energy minimisation, the steepest descent method is used. The maximum step size along a 0.01 nm gradient maximum of 50000 steps. Furthermore, the simulation system equilibrated at a continual temperature of 300 K, using the NVT and NPT ensemble simulation for processes for 100 ps. Initially, the modified Berendsen thermostat with no-pressure coupling was applied in the canonical ensemble of the NVT (constant number of particles, volume, and temperature). Then, the Parinello-Rahman method pressure of 1 bar (P) was applied in the NPT ensemble (constant number of particles, pressure, temperature). The final simulations were completed for each system for 10 ns, where a leap-frog integrator was applied for the trajectory time evolution (Amir *et al.*, 2019; Mazumdar *et al.*, 2020).

3.7 MD trajectories analysis

All trajectories were analysed by using trajectory analysis module integrated with the GROMACS 2020.01 simulation package, python, matplotlib, qtgrace, VMD and Chimera software. The trajectory files were first analysed by using GROMCAS tools, *gmx rmsd*, *gmx rmsf*, *gmx gyrate*, *gmx, S_{ASA}*, *gmx, hbond*, *gmx energy* for extracting the graph of root-mean-square deviation (RMSD), root-mean-square fluctuations (RMSFs), radius of gyration (Rg), solvent accessible surface area (S_{ASA}), hydrogen-bond, potential energy, kinetic energy, and enthalpy.

3.8 *C. beticola* *CbCyp51* gene copy number variation and expression analysis

Three experiments were performed to quantify *CbCyp51* gene expression and *CbCyp51* copy number variation analysis. Isolate S2 and S3 were chosen as the calibrator because they were displayed to have low *CbCyp51* gene expression and highly sensitive to propiconazole, prochloraz, and epoxiconazole in Table 4. First experiment liquid culture of R1, R2, R3, R4, R5, R6, R7, R8, R9, R10, R11, and R12 Resistance and two sensitive isolates above mentioned Table 4 were initiated by scraped mycelium from Potato dextrose agar (Himedia India) and put in into a 250 ml flask containing 50 ml of potato dextrose broth (Himedia India). Isolates were allowed to grow for 4 days, after which mycelium was harvested using cheesecloth and immediately stored at -80 °C. Genomic DNA was isolated from mycelium using GenElute™ Plant genomic DNA miniprep kit (Sigma-Aldrich Chemical Germany) following the manufacturer's instructions. In the second experiment, *CbCyp51* gene induction was measured in isolates with high EC50 values after being treated with propiconazole, prochloraz, and epoxiconazole at the equivalent of an EC50 of 10.0 µg/ml. To that end, liquid cultures of R1, R2, R3, R4, R5, R6, R7, R8, R9, R10, R11, and R12 Resistance and two sensitive isolates above mentioned Table 4 were performed as described above using a 250-ml flask containing 50 ml of potato dextrose broth (Himedia India). Each isolate was allowed to grow for 4 days, after which 50 µl of all three fungicides stock solution (10 mg/ml in DMSO) was added to the respective isolate to flask for a final concentration of 10.0 µg/ml. For comparison, sensitive and resistance isolate was also grown, as shown above, except 50 µl of DMSO was added in place of all three fungicides. Flasks were shaken (200 rpm) for 24 h at room temperature, after which mycelium was harvested using cheesecloth and immediately stored at -80 °C. Total RNA was isolated from mycelium using Hybrid-R™ kit (GeneAll Biotechnology Co., Ltd., Seoul, Korea) following the manufacturer's instructions. A High-Capacity cDNA Reverse Transcription Kit (Applied Biosystems™, US) was used to reverse-transcribe the RNA

templates. Relative *CbCyp51* copy number and *CbCyp51* expression experiments were performed in a CFX Connect Real-Time PCR Detection System (Bio-Rad Laboratories, Hercules, California, United States). gDNA (~13 ng) and cDNA (~13 ng) were used as templates for copy number variation and expression analysis, respectively. Actin was used as an internal standard (Bolton, Birla, Rivera-Varas, Rudolph, & Secor, 2011). Gene-specific primers (GSPs) for quantitative real-time PCR conduct experiments are listed in Table 3. The results were calculated using the $2^{-\Delta\Delta C_t}$ method (Sen *et al.*, 2021), and a comparison between the S and R biotypes was performed using a two-sample t-test.

Table 3: List of primers used in this study. Primer pairs RT_F1-RT_R1 and RT_F2-RT_R2 were used in copy number variation and gene expression analysis. Primer pairs F1-R1 and F2-R2 and cloning_F1- cloning_R1 and cloning_F2- cloning_R2 were used to isolate and clone partial *CbCyp51* gene from *C. beticola*.

Name	Sequence (5' to 3')	Melting Temp. (°C)	Amplicon Length (bp)
F1	GTGTTTGGCAAGGACGTCG	62	644
R1	TGTTCCCTGCACAAGCTCATC		
F2	TCAGAGAACGGAGAGGAGGA	63	788
R2	CTCTCCCCTTCACAACAGC		
RT_F1	TCGTCTTCCACTTCGTACCC	58	172
RT_R1	CCGTTTCAGGATGAAGTCGTT		
RT_R1	ACAGGAGACGCGATTATGCT	60	155
RT_F1	GATAGGCGTGCCATCTTTGT		
RT_Actin F1	ACGGAGTTACCCACGTTGTC	58	174
RT_Actin R1	TCTCCTTGATGTCACGAACG		
RT_Actin F2	ACGTCACCACCTTCAACTCC	58	172
RT_Actin R2	GGTGCGATGATCTTGACCTT		
Cloning_F1	TCGTCTTCCACTTCGTACCC	60	1453
Cloning_R1	CTCTCCCCTTCACAACAGC		
Cloning_F2	GTGTTTGGCAAGGACGTCG	61	1229
Cloning_R2	CTCTCCCCTTCACAACAGC		

3.9 RNA extraction, RNAseq library preparation and Illumina sequencing.

Total RNA was extracted from frozen mycelium tissues of *C. beticola* isolates Cb-Resistance and Cb-Sensitive using GeneAll® RiboEx™ (GeneAll Biotechnology; Seoul; South Korea) following the manufacturer's instructions. The total RNA qualities were further analysed using Qubit 4 Fluorometer (Thermo Fisher; Massachusetts; USA), and integrity of total RNA was checked in agarose gel Figure 6 shows below. Final quality and RNAseq library prepared by Novogene (Novogene, China). Five biological replications of each genotype per time-point were used for 150 bp paired-end RNA-seq sequencing (Novogene, China) with Illumina HiSeq 4000 sequencing system (Novogene, China).

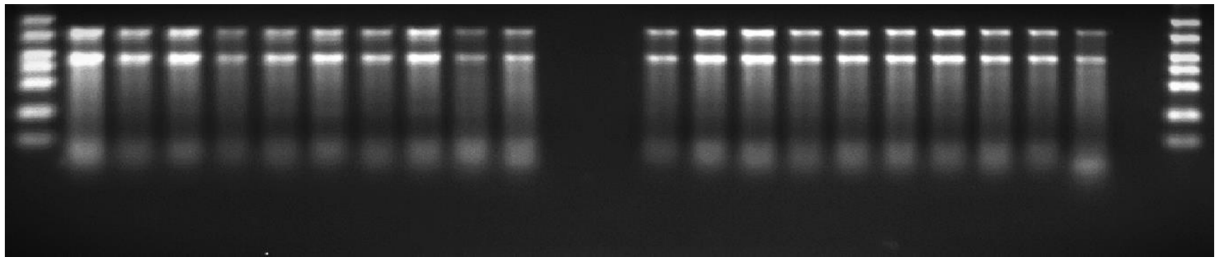


Figure 6 Total RNA integrity of all *C. beticola* isolates Cb-Resistance and Cb-Sensitive tested in agarose gel before samples were sent for transcriptome sequencing.

3.10 RNAseq Analysis of resistant and sensitive isolates

Two biological replicates were sequenced for resistant and sensitive isolates with treated and non-treated. Each biological replicate had five technical replicates. There were 20 experimental units, each with a minimum of 1,500,000 total RNA-Seq reads. The following techniques in this section were performed using the OmicsBox software (BioBam Bioinformatics; Valencia; Spain). Raw RNA-Seq reads were transformed into FASTQ file format, read quality was evaluated, and poor reads were cleaned out using the default parameters of FastQC version 0.11.9 (Andrews, 2010). All RNA-Seq reads that meet the quality of threshold for resistant and sensitive isolates were, respectively, aligned to the resistant and sensitive isolate's reference genomes of *C. beticola* using software STAR aligner in the OmicsBox (Dobin *et al.*, 2013). Only one mismatch between the RNA-Seq read and the reference genome was allowed, and reads were permitted to match with only one region in the genome. These stringent mapping factors were used to diminish the likelihood of false matching between predicted genes and RNA reads.

Using the edgeR package to inbuild the OmicsBox environment and our count tables, separate differential expression analyses were run for sensitivity and Resistance (Robinson *et al.*, 2010). In both

instances, read count per million (CPM) filter was set to the least one sample needed to reach this standard. These parameters suggested that, for each million reads in a technical replicate, at least one has to map to a particular gene to be included in the analysis. On average, there were between two and three million reads mapped to a reference genome of *C. beticola*. Thus, for a particular gene to be included in the analysis. Since there were many genes whose samples possessed fewer matches, this standard was considered suitable for acquiring consistent calculations of gene differential expression. However, we ran each differentially expressed gene contrary to the Conserved Domain Search tool of NCBI to further verify the gene's functions and non-matching genes were described as encoding a hypothetical protein. GO annotation counts for the differentially expressed genes in resistant, sensitive, and non-treated isolates.

3.11 Identification of Ergosterol Biosynthesis Genes

A list of supposed ergosterol biosynthesis genes was obtained from our annotated *C. beticola* genome using the GO term ergosterol biosynthetic process. NCBI protein blast was also performed against the *C. beticola* genome using various NCBI reference ergosterol biosynthesis genes from *C. beticola*. This step was completed to try and capture supposed ergosterol biosynthesis genes lacking from our GO term search. We used the pathway discussed by (Bolton *et al.*, 2016) to help us guide our NCBI gene search.

Chapter: 4 Results

4.1 Sample collection and fungicide sensitivity

Twelve resistant isolates (from R1 to R12, resistant to propiconazole, prochloraz and epoxiconazole, shown in Table 5) and two susceptible isolate S2 and S3 were screened out from two fifty isolates from 2018-2020, shown in Table 5. All three fungicides (propiconazole, prochloraz and epoxiconazole) were effective against S2 and S3. The EC50 value is shown in Table 5, the resistance factor (RF) for S2 is shown in table 6 and the S3 resistance factor is shown in Table 7 for all resistance biotypes. Calculation of resistance factor to S2 with resistance biotype against propiconazole was R3 (693X), R6 (464X), R2 (462X) and R1 (426X) fold resistance were found whereas, against S3, R3 (787X), R6 (528X), R2 (525X) and R1 (484X) fold resistance found shown in Table 6 and Table 7. Resistance factors were calculated to S2 sensitive isolate against prochloraz resistance isolate, which shows R4 (1692X), R5 (1475X), R12 (1364X) and R9 (1300X) whereas against S3 resistance factor was R4 (9517X), R5 (8293X), R12 (7672X) and R9 (7310X) shows in Table 6 and Table 7. Calculation of resistance factor to S2 with resistance biotype against epoxiconazole was R8 (12974), R11 (7154X), R10 (6917X) and R7 (6337X) fold resistance were found whereas, against S3, R8 (3866), R11 (2132X), R10 (2061X) and R7 (1888X) fold resistance found shown in Table 6 and Table 7.

Table 4 Fungicide sensitivity assays. Top 20 sensitive and resistant isolates of out 250 were screened against 3 DMIs fungicides, e.g. propiconazole, prochloraz and epoxiconazole. EC50 values were calculated using graph pad prism software (9.0.0), based on each isolate's mean colony diameter and radial growth, and all EC50 values are in µg/ml.

Biotype	Prochloraz		Propiconazole		Epoxiconazole	
	EC50 (Mean value)	SD	EC50 (Mean value)	SD	EC50 (Mean value)	SD
S2 (7A_4)	0.06	0.02	0.09	0.01	0.05	0.01
S5 (4_2)	0.10	0.04	0.08	0.02	0.05	0.03
R4 (31_4)	15.43	0.07	0.38	0.07	0.33	0.03
R6 (63_2)	0.18	0.04	13.86	0.97	0.26	0.03
R11 (M68_3)	0.62	0.13	0.12	0.04	25.34	1.88
ST_1	2.23	0.43	1.97	0.28	1.01	0.12
ST_2	2.25	0.79	2.39	0.45	1.22	0.09
ST_3	2.11	1.07	2.88	2.02	0.81	0.10
ST_4	1.59	0.30	0.60	0.18	0.65	0.12
ST_5	1.40	0.33	1.15	0.27	1.22	0.33
ST_6	1.54	0.27	2.90	1.09	0.61	0.02
ST_7	0.71	0.30	0.67	0.36	0.51	0.12
ST_8	1.67	0.32	1.94	0.19	4.66	0.40
7B_1	0.76	0.13	0.88	0.03	1.17	0.31
7B_2	1.28	0.10	0.86	0.08	1.38	0.19
7B_3	1.14	0.28	1.55	0.24	1.54	0.36
7B_4	1.01	0.25	0.66	0.03	1.71	0.34
VM72_1	ND	ND	0.16	0.01	1.02	0.06
VM72_2	1.10	0.03	0.52	0.11	0.42	0.04
VM72_3	2.00	0.97	0.38	0.15	1.05	0.04
VM72_4	0.58	0.09	0.31	0.24	2.37	0.23
VM72_5	2.95	0.73	0.40	0.10	2.82	0.32
A_1	0.62	0.07	0.18	0.06	1.47	0.67
A_2	1.11	0.21	0.13	0.01	1.11	0.04
A_3	0.36	0.04	0.16	0.04	1.41	0.09
A_4	0.33	0.12	0.50	0.03	1.14	0.16
B_1	0.55	0.03	0.31	0.03	1.06	0.02
B_2	0.60	0.04	0.58	0.03	0.18	0.02
B_3	0.22	0.04	0.22	0.02	0.50	0.04
B_4	0.13	0.01	0.35	0.01	0.60	0.07
B_5	0.48	0.12	0.36	0.08	1.36	0.14
C_1	1.34	0.25	1.50	0.29	2.81	0.63
C_2	0.36	0.19	0.36	0.24	0.88	0.13

C_3	1.16	0.12	0.30	0.02	0.86	0.14
C_4	1.33	0.03	1.95	0.41	1.10	0.30
C_5	2.02	0.09	1.34	0.32	1.45	0.14
D_1	1.90	0.33	1.23	0.16	0.76	0.08
D_2	1.27	0.06	1.24	0.51	0.61	0.06
D_3	1.41	0.12	ND	ND	0.61	0.16
D_4	1.65	0.07	0.36	0.08	0.88	0.07
D_5	1.51	0.08	0.65	0.33	1.26	0.25
E_1	1.30	0.09	1.06	0.29	1.43	0.12
E_2	0.26	0.00	1.76	0.29	0.83	0.02
E_3	0.34	0.02	0.97	0.41	0.52	0.02
E_4	0.29	0.00	1.30	0.44	1.84	0.26
E_5	0.22	0.01	1.30	0.24	ND	ND
M61_1	0.33	0.02	0.97	0.19	2.19	0.68
M61_2	0.24	0.01	0.83	0.18	0.65	0.09
M61_3	0.36	0.02	1.06	0.33	0.27	0.02
M61_4	0.32	0.02	0.64	0.12	1.05	0.53
M61_5	0.70	0.02	2.51	0.57	0.43	0.09
28_1	0.56	0.05	2.45	0.78	1.69	0.24
28_2	0.40	0.02	ND	ND	1.34	0.15
7B_1 (S3)	0.19	0.02	0.17	0.02	0.05	0.01
1_6 (S4)	0.32	0.22	0.05	0.01	0.45	0.32
ST_8 (R2)	2.29	0.23	14.27	2.94	2.19	0.17
36_2 (R5)	44.01	5.85	5.43	0.54	2.78	0.13
M61_5 (R10)	4.34	0.42	3.11	0.14	39.53	6.23
7A_2	1.36	1.05	1.98	1.21	2.06	0.64
7A_3	1.22	0.04	2.06	0.56	1.14	0.93
7A_4	1.81	1.52	1.53	1.09	1.52	0.51
7A_5	1.29	0.59	ND	ND	1.61	0.35
3_2	0.90	0.54	1.96	0.65	5.72	8.22
3_3	1.24	1.00	1.17	0.25	1.06	0.70
3_4	2.71	1.54	1.10	0.80	ND	ND
3_5	0.62	0.54	0.47	0.37	1.18	0.34
4_2	1.84	0.92	1.48	0.22	ND	ND
4_3	1.13	0.19	1.53	1.24	0.84	0.40
4_4	0.24	0.08	0.61	0.53	1.29	0.35
5_2	1.22	0.62	2.05	0.94	1.49	1.19
5_3	1.47	0.66	1.48	0.38	1.06	0.51
5_4	0.95	0.68	0.98	0.90	1.47	0.20
5_5	0.35	0.25	0.75	0.34	1.22	0.50
vs_1	1.04	0.15	0.87	0.22	7.60	11.16
vs_2	0.97	0.27	ND	ND	3.99	3.46

vs_3	ND	ND	1.17	0.51	4.92	5.94
8_1	ND	ND	2.39	1.29	2.37	1.06
8_2	1.06	0.37	2.68	1.51	1.24	0.37
8_3	1.04	0.12	1.45	0.96	1.20	0.79
9_1	2.03	0.90	0.98	0.57	ND	ND
9_2	1.32	0.27	1.15	1.01	1.11	0.79
9_3	1.12	0.82	1.14	0.95	1.15	0.59
11_1	1.29	0.39	0.92	0.70	1.06	0.41
11_2	ND	ND	2.80	1.44	1.43	0.73
11_3	1.30	0.40	1.50	1.32	1.88	0.15
17_1	1.46	0.91	1.42	1.03	1.41	1.13
17_2	1.25	0.54	1.30	0.98	1.50	0.71
17_3	1.49	0.70	0.31	0.29	1.72	1.26
20_1	ND	ND	0.97	0.46	1.19	0.30
23_1	1.12	0.69	0.50	0.57	1.42	0.91
24_1	1.22	0.68	1.02	0.66	0.54	0.45
25_1	2.54	0.95	0.77	0.78	1.23	0.85
70_5	1.21	0.50	0.53	0.44	1.41	0.57
70_1	1.86	0.23	0.57	0.41	1.47	0.95
70_2	0.71	0.46	ND	ND	1.12	0.42
72_1	1.29	1.07	1.79	1.26	1.30	0.42
73_1	0.91	0.83	0.62	0.49	0.93	0.73
E_1	1.91	0.77	1.47	1.98	0.50	0.38
E_2	1.01	0.34	0.68	0.45	0.95	0.47
E_3	1.02	0.26	0.80	0.91	0.57	0.46
E_4	1.01	0.26	1.75	0.52	0.96	0.83
E_5	0.89	0.92	1.35	0.49	0.91	0.64
M61_1	0.97	0.56	0.83	0.95	1.13	0.72
M61_2	0.88	0.49	1.48	0.43	ND	ND

#ND: “not done”.

#S: sensitive biotype

#R: resistant biotype

Table 5 Effective concentration at 50% (EC50) for *C. beticola* isolates collected from 2018-22. A fungicide sensitivity assay against two fifty isolates was performed, and from screening, four highly resistant and two sensitive isolates for each fungicide.

EC50 µg/ml					
Propiconazole		Prochloraz		Epoxiconazole	
S2	0.21	S2	0.38	S2	0.06
S3	0.19	S3	0.07	S3	0.21
R3	148.30	R4	643.80	R7	801.80
R6	99.44	R5	561.00	R8	442.10
R2	98.96	R12	519.00	R10	427.50
R1	91.27	R9	494.50	R11	391.60

Table 6 Resistance factor against S2 of all resistance biotypes for all three DMIs fungicides.

The resistance factor to S2					
Propiconazole		Prochloraz		Epoxiconazole	
R3	693	R4	1692	R8	12974
R6	464	R5	1475	R11	7154
R2	462	R12	1364	R10	6917
R1	426	R9	1300	R7	6337

Table 7 Resistance factor against S3 of all resistance biotypes for all three DMIs fungicides.

The resistance factor to S3					
Propiconazole		Prochloraz		Epoxiconazole	
R3	787	R4	9517	R8	3866
R6	528	R5	8293	R11	2132
R2	525	R12	7672	R10	2061
R1	484	R9	7310	R7	1888

4.2 Artificial inoculation

An artificial inoculation experiment was performed on a sugar beet plant for CLS disease pathogen *C. beticola* in-vitro conditions in growth chamber. When one resistance and one sensitive biotype were sprayed on the resistance and susceptible cultivars. The first symptoms appeared on susceptible and resistant cultivars on 9th day after inoculation with S and R biotypes. However, infection increased on the susceptible cultivar, whereas on the resistance cultivar, symptoms remained stable on the 11th and 14th day; no further upsurge in visible symptoms is shown in Figure 7. After the 16th and 18th, symptoms significantly increased compared with the resistance cultivar. However, leaves with visible symptoms were processed for Koch's postulates criteria designed to prove the causative association of *C. beticola* in sugar beet with PCR.

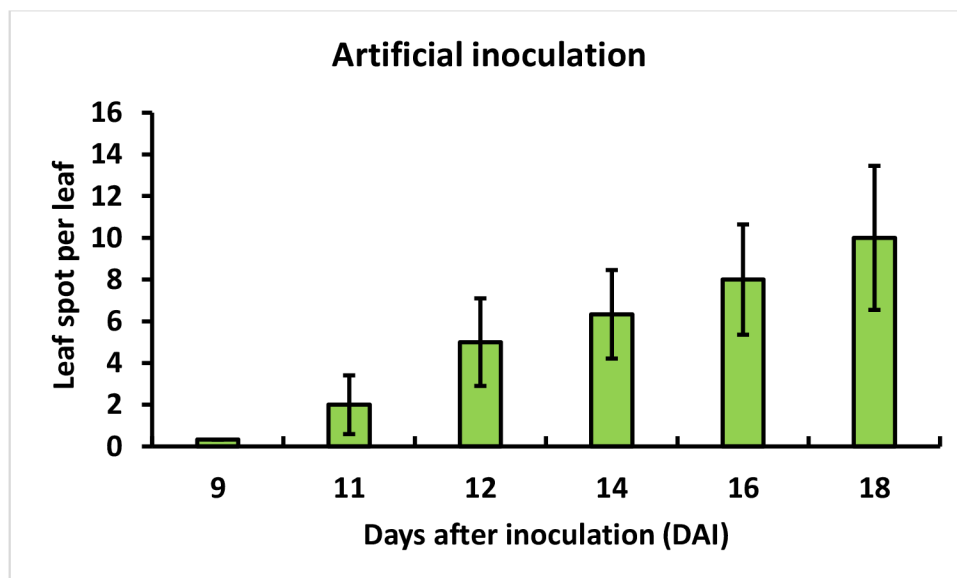


Figure 7 Artificial inoculation of *C.beticola* in a susceptible sugar beet cultivar at various times after inoculation in growth chamber and leaf spot symptoms counted per leaf on DAI.

4.3 *Cercospora beticola* *CbCyp51* gene mutations

The primer pair's cloning_F1 & cloning_R1, cloning_F2 & cloning_R2 resulted in 1453 bp and 1229 bp amplicons, respectively. The PCR products were evaluated in a 1% agarose gel, where a single band was obtained for each primer pair (data not shown). Partial amplification of the *C. beticola* 14 α demethylase gene with the above-mentioned primers detected the mutation Table 8 in all the resistant isolates compared with S2 and S3 and the *CbCyp51* wild-type isolate CVA41 (GenBank Acc. No. KU665583.1).

Table 8 Result of *CbCyp51* mutation amino acid change in *CbCyp51* in comparison with wild type and isolate CVA41 from NCBI (GenBank Acc. No. KU665583.1).

Isolate	mutation
S2	NA
S3	NA
R1	Y464S
R2	Y464S
R3	Y464S
R4	Y464S
R5	Y464S
R6	I387M
R7	Y464S
R8	Y464S
R9	Y464S
R10	Y464S
R11	I309T
R12	Y464S

4.4 *C. beticola* *CbCyp51* gene copy number variation and expression analysis

No significant relative *CbCyp51* gene copy number variation or change in *CbCyp51* gene expression was detected for the R1, R9 and R10 biotypes, compared with S3 and S4, which indicates that gene amplification and overexpression are not involved in the resistance against propiconazole, prochloraz and epoxiconazole Figure 8 and Figure 9. However, in R2, R4 and R8 significant increase in the target gene copy number was observed compared to S3 and S4 Figure 9. Additionally, comparative *CbCyp51* gene expression data indicated that the *CbCyp51* gene in the R3, R5, R6, R7, R8, and R12 biotypes was overexpressed compared to that in the S3 and S4 biotypes Figure 8. However, in R1, R9 and R10 biotypes, no *CbCyp51* gene copy number variation and gene expression have been significantly different compared to S3/S4 and fungicide induced Figure 8 and Figure 9.

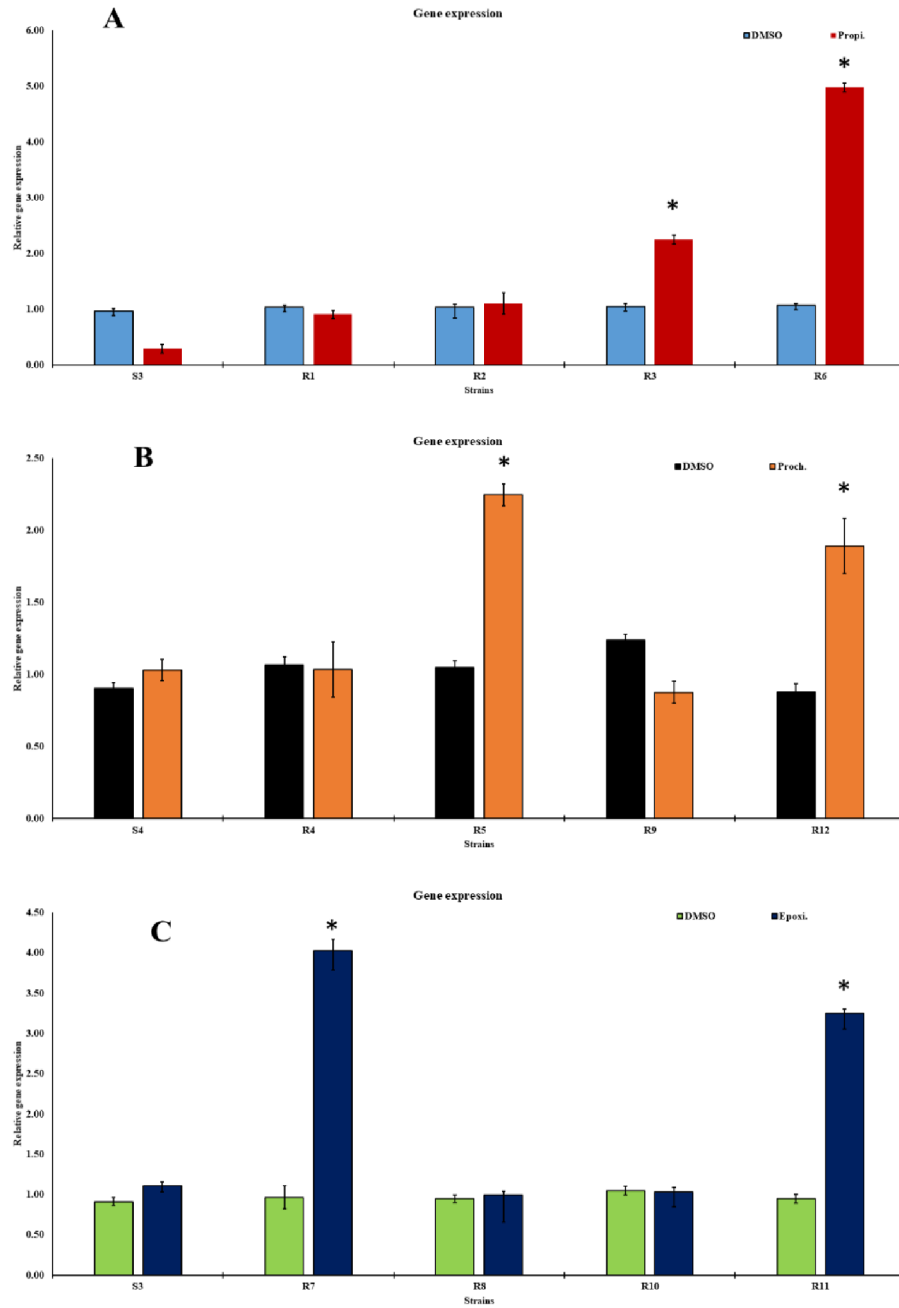


Figure 8 Analysis of relative gene expression. The relative gene expression values are in terms of $2^{-\Delta\Delta C_t}$ values. (A) Relative gene expression level between the treated and non-treated S3 and Resistance strain with propiconazole and DMSO. (B) Relative gene expression level between the treated and non-treated S4 and Resistance strain with prochloraz and DMSO. (C) Relative gene expression level between the treated and non-treated S3 and Resistance strain with epoxiconazole and DMSO.

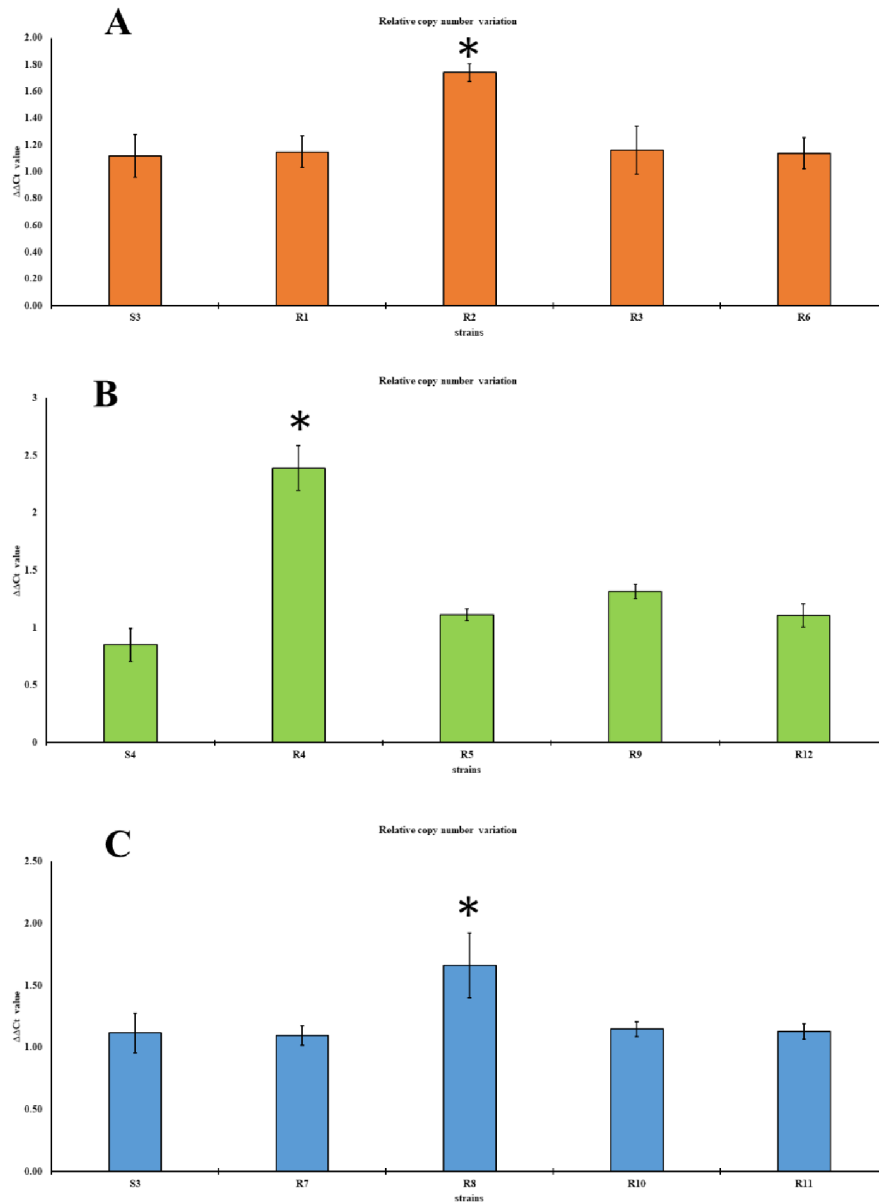


Figure 9 Analysis of copy number variation. The relative copy number values are in terms of $2^{-\Delta\Delta C_t}$ values. “*” denotes significance at 5% significant level. (A) Copy number variation in difference between S3 and R2 at the 5% significant level. (B) Copy number variation in difference in only R4 compared with S2; however, R6 and R11 were not found any significant difference at the 5% significance level.

4.5 *Cercospora beticola* CbCyp51 protein structure validation

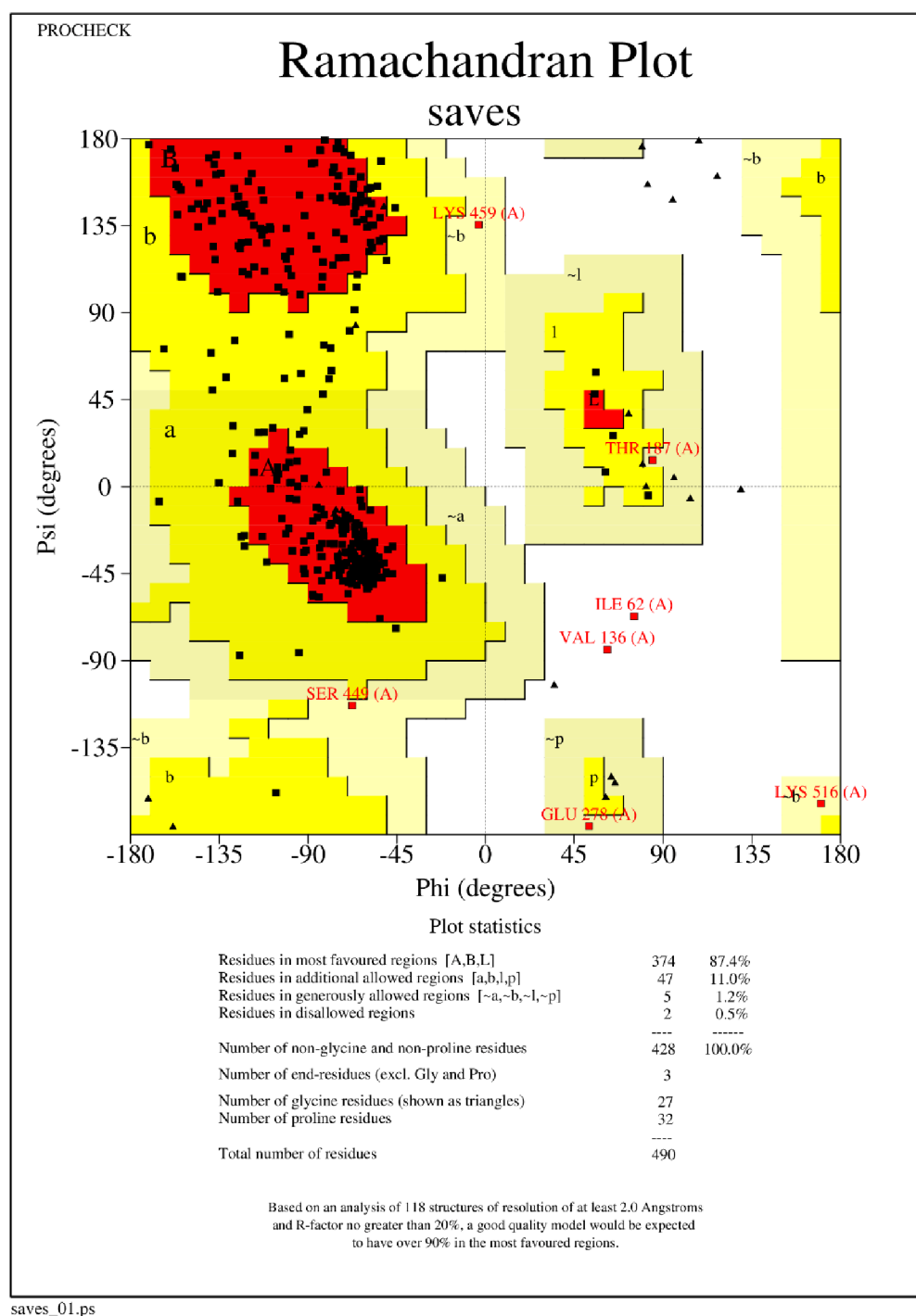
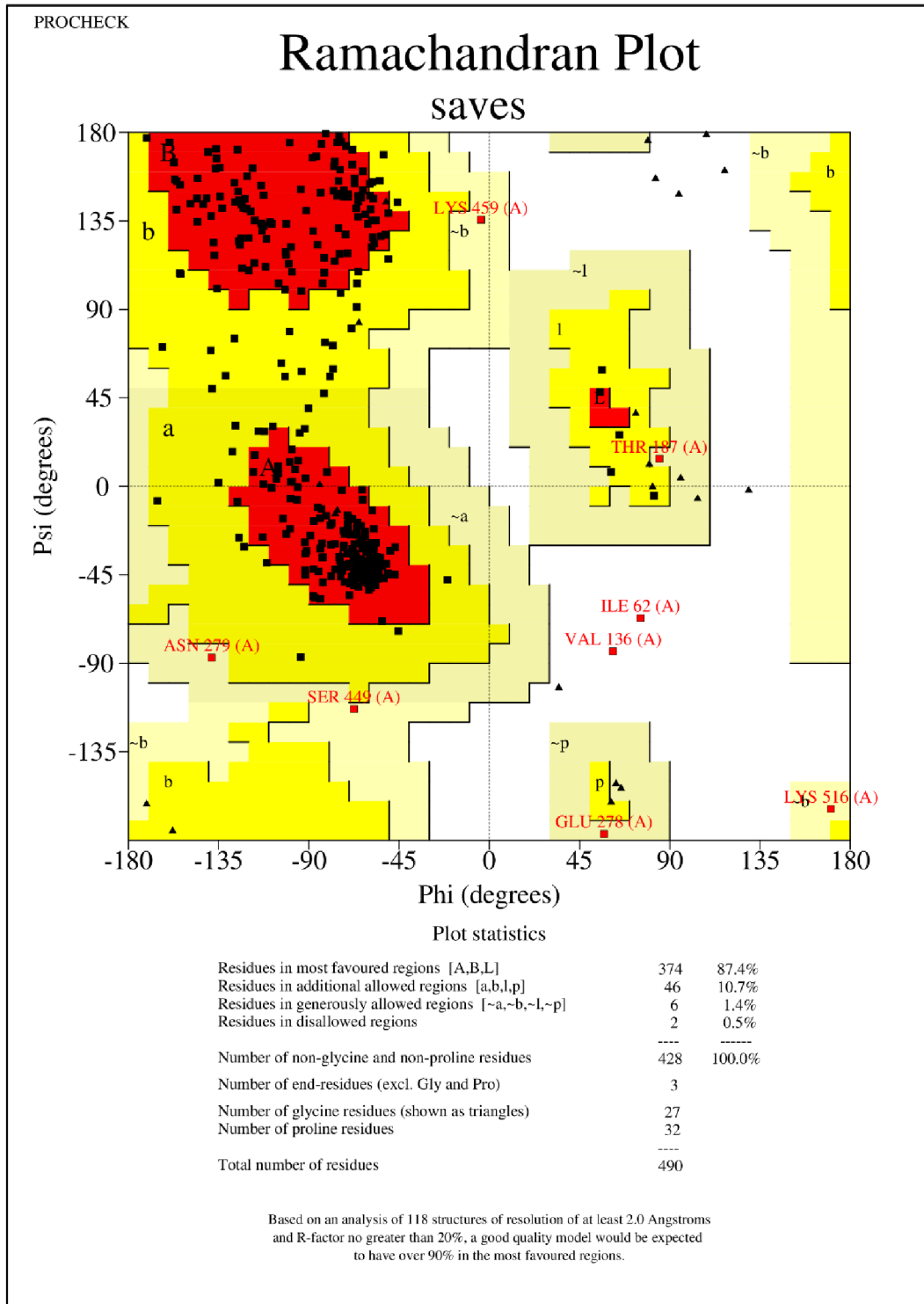
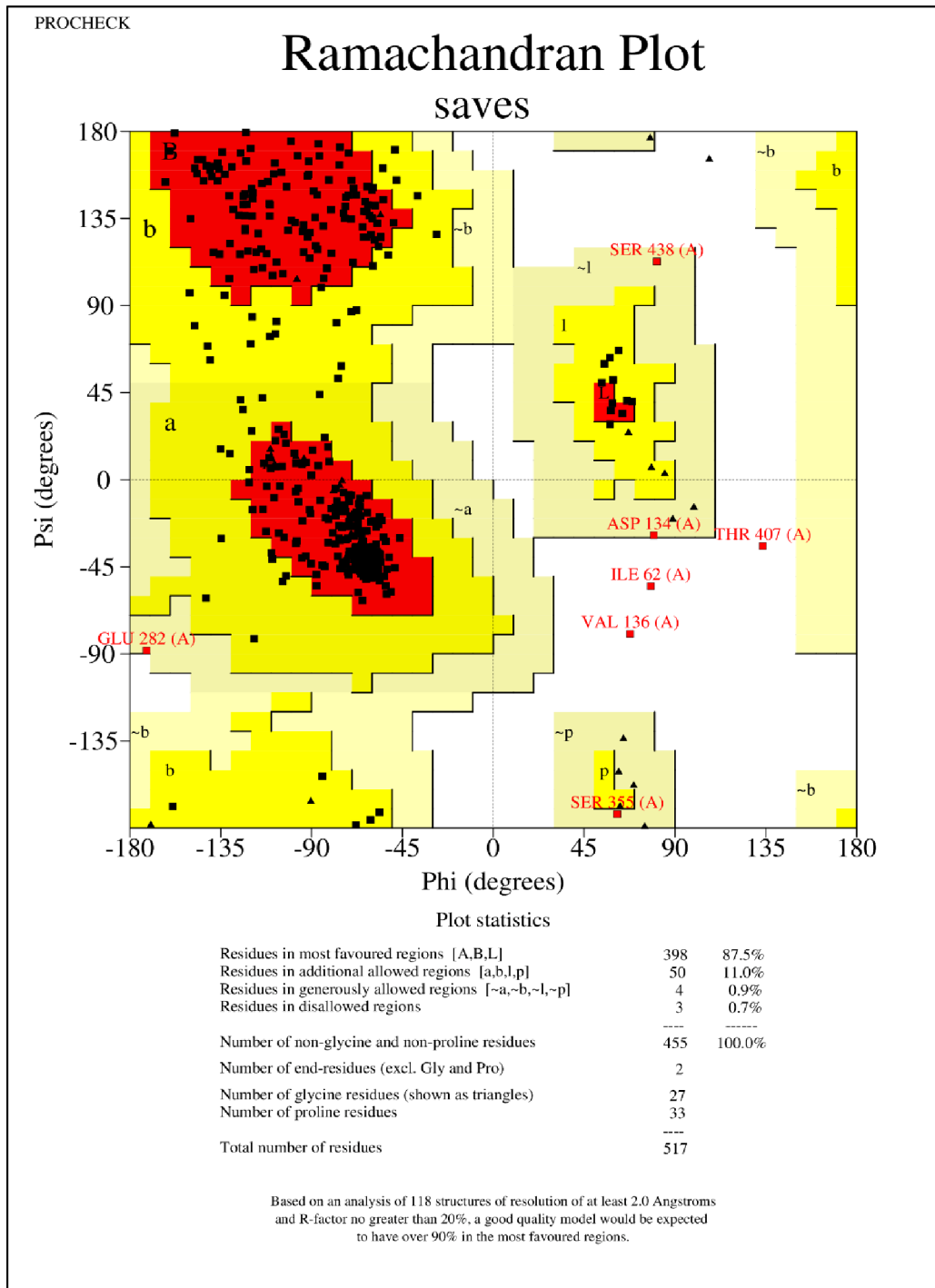


Figure 10 Structure validation parameter Ramachandran plot of Sensitive biotypes S2 and S3 without any mutation.



saves_01.ps

Figure 11 Structure validation parameter Ramachandran plot of resistance biotype with mutation Y464S.



saves_01.ps

Figure 12 Structure validation parameter Ramachandran plot of resistance biotype with mutation I387M.

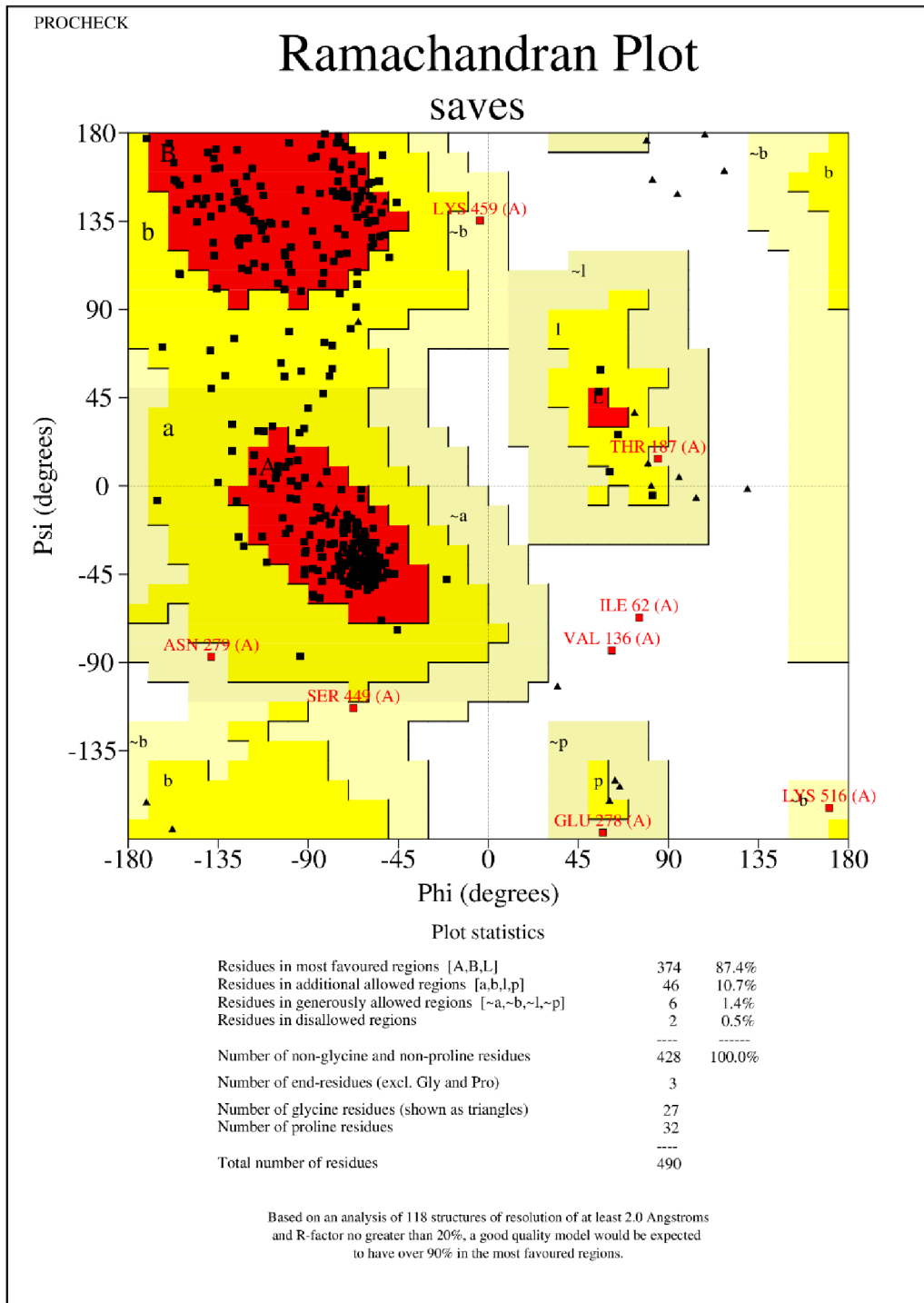


Figure 13 Structure validation parameter Ramachandran plot of resistance biotype with mutation I309T.

4.6 Impact of the Y464S mutation on propiconazole binding

4.6.1 Molecular docking studies

The molecular structure of the interaction between propiconazole and the wild type (WT) and mutant type (MT) *CbCyp51* is shown in Figure 14. Molecular docking studies revealed that binding affinity values for the WT and MT were -7.4 kcal/mol and -6.8 kcal/mol, respectively Figure 15. Eighteen amino acids were predicted to be directly involved in propiconazole binding in the *CbCyp51* WT-fungicide interaction. However, for *CyCyp51* MT-fungicide interaction, fewer amino acids (only eleven) were predicted to be involved in propiconazole binding. No amino acids were involved in hydrogen bonding in either case.

Moreover, our analysis detected seven interacting amino acids (Thr127, Tyr137, Lys148, Ala310, Ile384, His483 and Phe526) involved in the wild type but absent in the *CbCyp51* MT. These amino acids might play essential roles in fungicide binding. However, this finding requires further validation. Secondary structure analysis showed an increased percentage of alpha helixes and a decreased percentage of beta-strands and random coils in the *CbCyp51* MT-fungicide complex compared to the *CbCyp51* WT-fungicide complex Figure 15. Detailed changes in the secondary structure of the *CbCyp51* protein in the presence of ligands for both the WT and MT are shown in Figure 17.

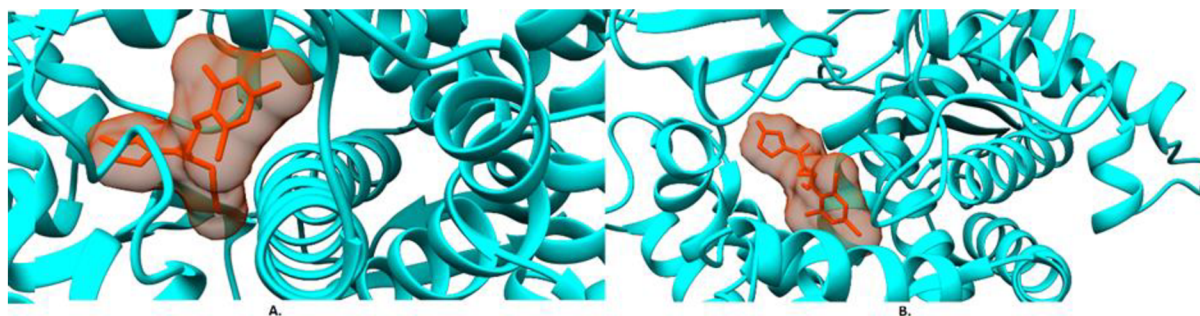


Figure 14 Interaction between propiconazole and the *CbCyp51* protein molecular structure of wild type (A.) and the mutant type (B.).

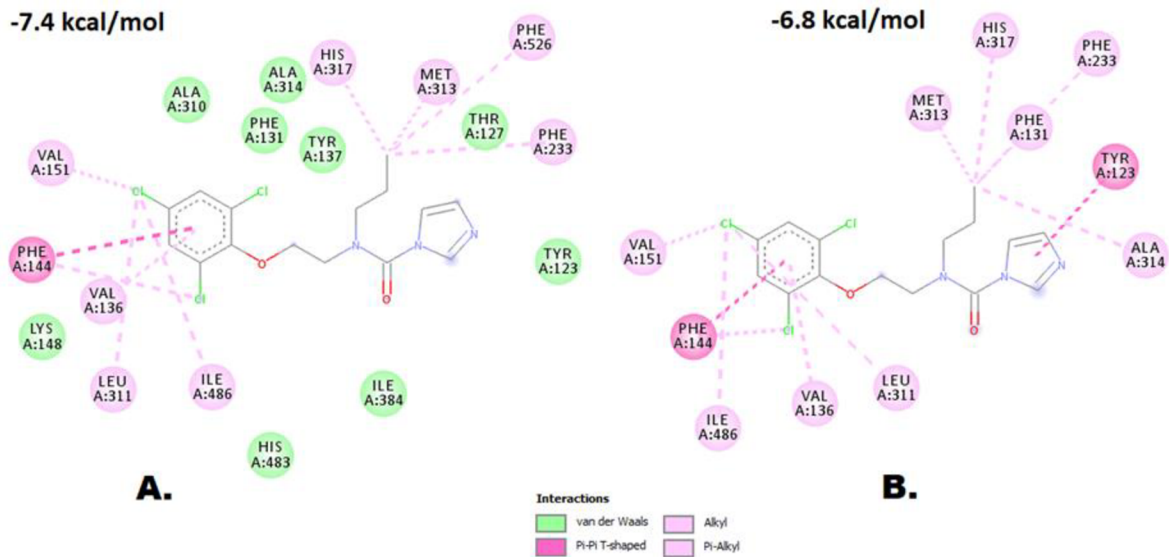


Figure 15 Results for interacting amino acids. (A) *Cb_CbCyp51_WT* and propiconazole binding, (B) *CbCyp51* MT and propiconazole binding. The mentioned values in the figures are binding affinity values.

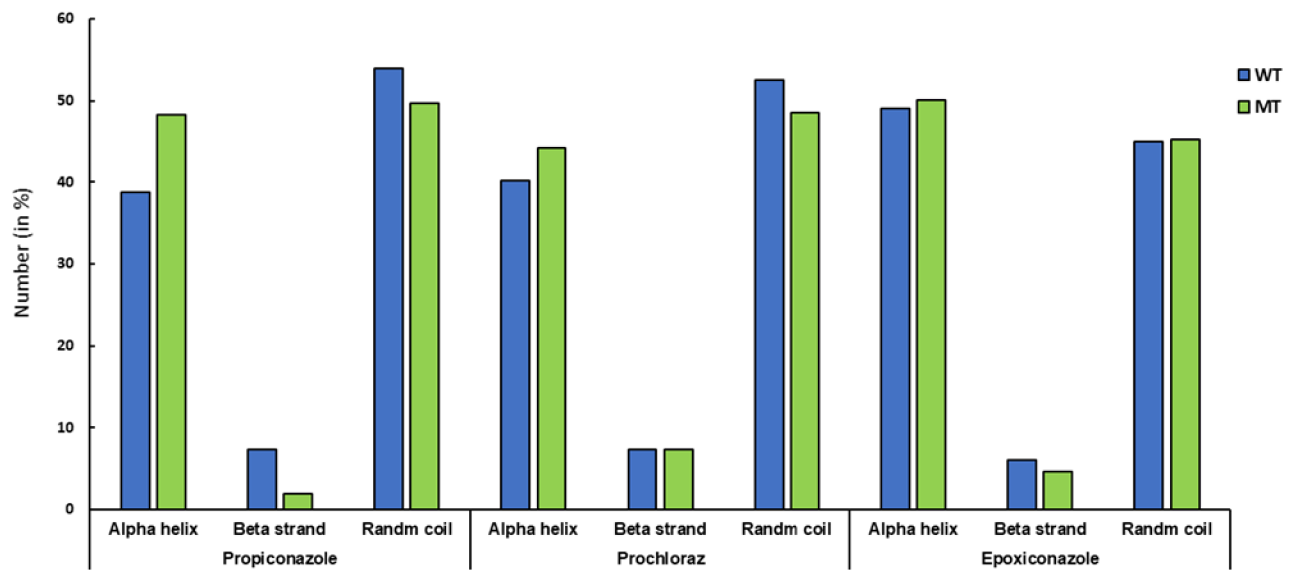


Figure 16 Results for secondary structure analysis during protein-ligand interaction.

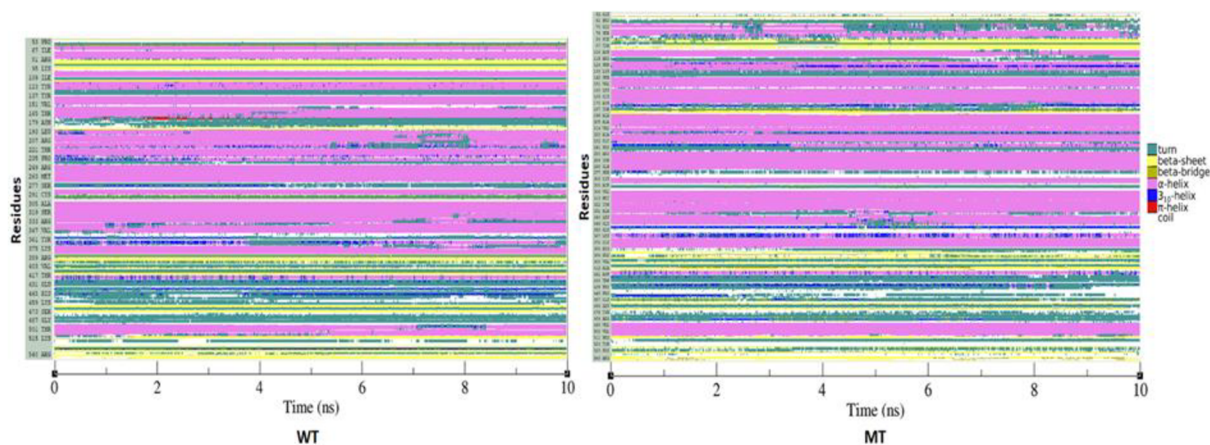


Figure 17 Change in the secondary structure of *CbCyp51* protein of R2 (MT) with comparison S3 (WT) biotype, which is resistant to propiconazole.

4.6.2 Behavioural dynamics of the wild-type and mutant-type systems

Protein-ligand RMSD values for the wild and the mutant are shown in Figure 18. The molecular dynamics simulation of the *CbCyp51* WT fungicide and *CbCyp51* MT fungicide systems was carried out for 10 ns to elucidate the resistance mechanism further. The root mean square fluctuation (RMSF) versus residue number was also calculated to measure the mobility of residues during simulation. Varying fluctuations of the residues were detected when the MT was compared to the WT Figure 19. In addition, the S_{ASA} area was calculated for the MT and WT when they were bound to their ligands. Our results showed that for the *CbCyp51* WT-fungicide interactions, S_{ASA} was ~ 235 nm². However, for the *CbCyp51* MT-fungicide interaction, a slight increase in the S_{ASA} (~ 245 nm²) was detected in Figure 20. The possible explanation for this finding might be a slight change in the conformation of the *CbCyp51* protein, which might have occurred due to the Y464S mutation.

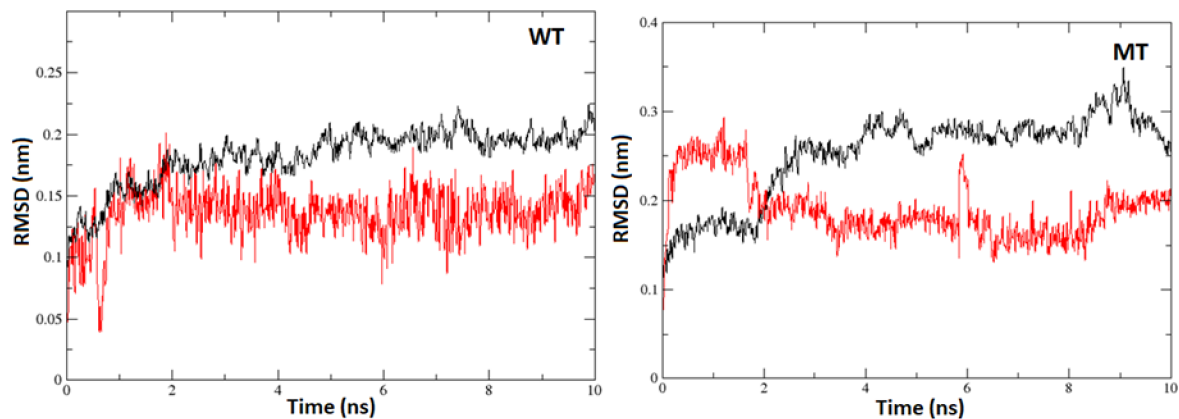


Figure 18 *CbCyp51* protein and propiconazole (ligand) root mean square deviation (RMSD) value of S3 (WT) and R2 (MT) biotype.

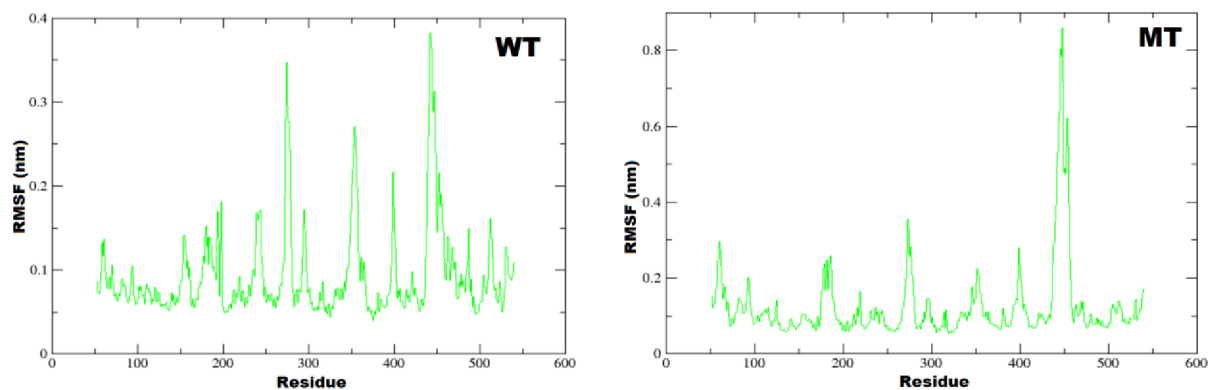


Figure 19 Residue-wise root mean square fluctuation values during propiconazole *CbCyp51* interaction.

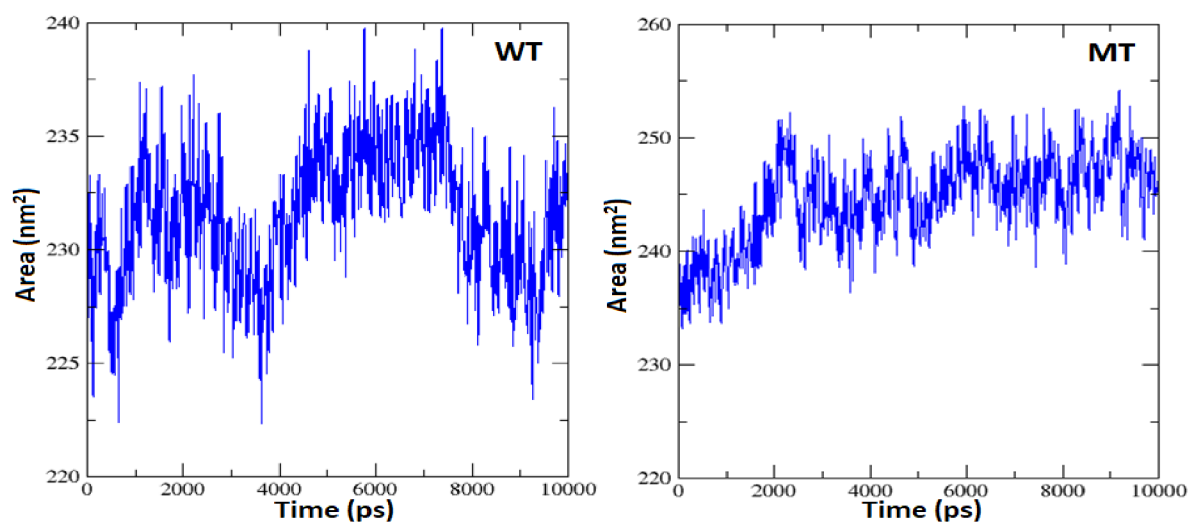


Figure 20 Solvent accessible surface area analysis during propiconazole *CbCyp51* interaction.

4.7 Impact of the Y464S mutation on prochloraz binding

4.7.1 Molecular docking studies

The molecular structure of the interaction between prochloraz and the wild-type (WT) and the mutant-type (MT) *CbCyp51* is shown in Figure 21. Molecular docking studies revealed that the binding affinity values for the WT and the MT were -7.6 kcal/mol and -7 kcal/mol, respectively (Figure 22). Five amino acids (Phe238, Leu126, Ile387, Ile384 and Tyr137) were predicted to be directly involved in prochloraz binding, irrespective of WT or MT. These amino acids might play important roles in prochloraz binding. Tyr137 was found to be involved in hydrogen bonding in both cases. Thus, it can be concluded that the protein-ligand conformation was not affected by the Y464S mutation. However, secondary structure analysis showed that in the case of the *CbCyp51* MT-fungicide complex, the percentages of alpha helices and random coils were higher and lower, respectively, than those of the *CbCyp51* WT-fungicide complex. Interestingly, no change in the percentage of beta strands was detected in Figure 16. Detailed changes in the secondary structure of the *CbCyp51* protein in the presence of ligands for both the WT and MT are shown in Figure 23.

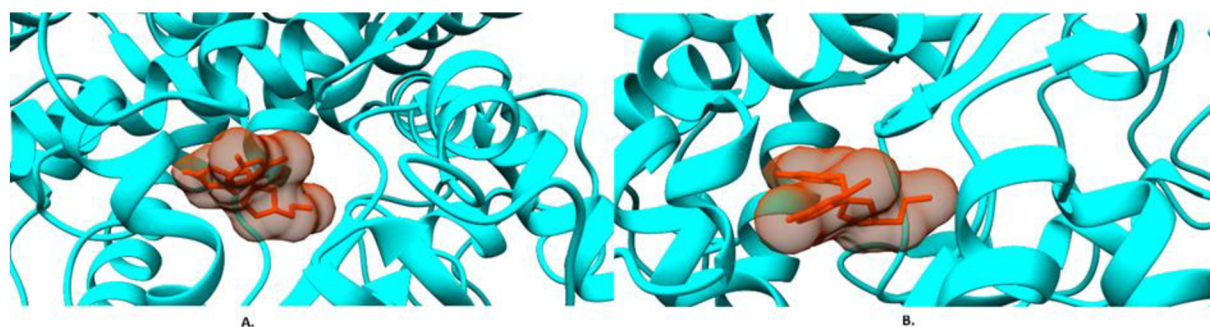


Figure 21 Interaction between prochloraz and the *CbCyp51* protein molecular structure of wild type (A) and the mutant type (B)

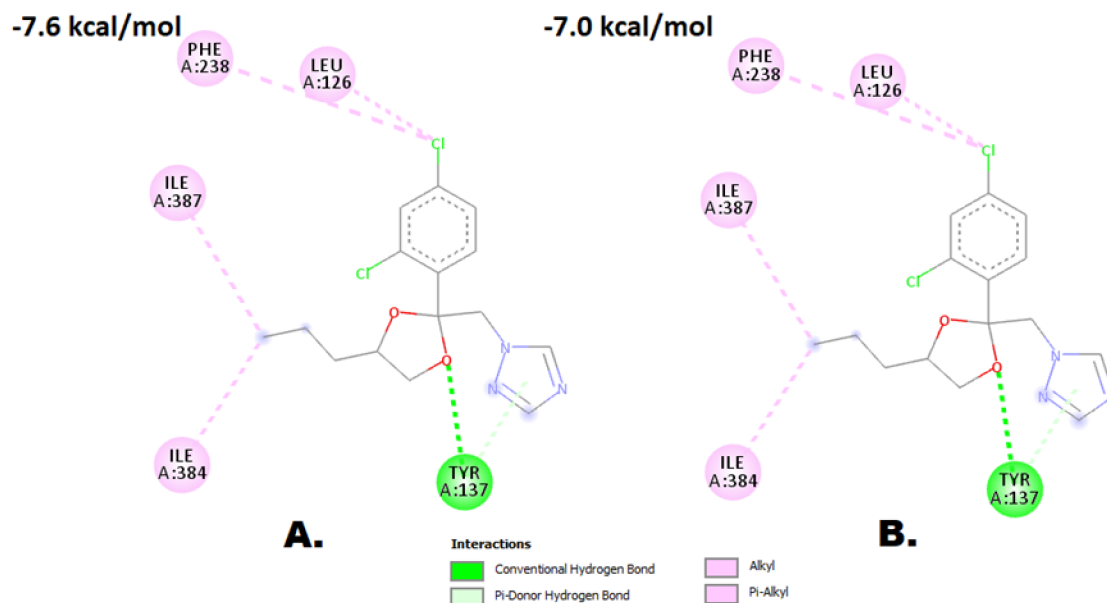


Figure 22 Results for interacting amino acids. A. *CbCyp51* WT and prochloraz binding (B) *CbCyp51* MT and prochloraz binding. The mentioned values in the figures are binding affinity values.

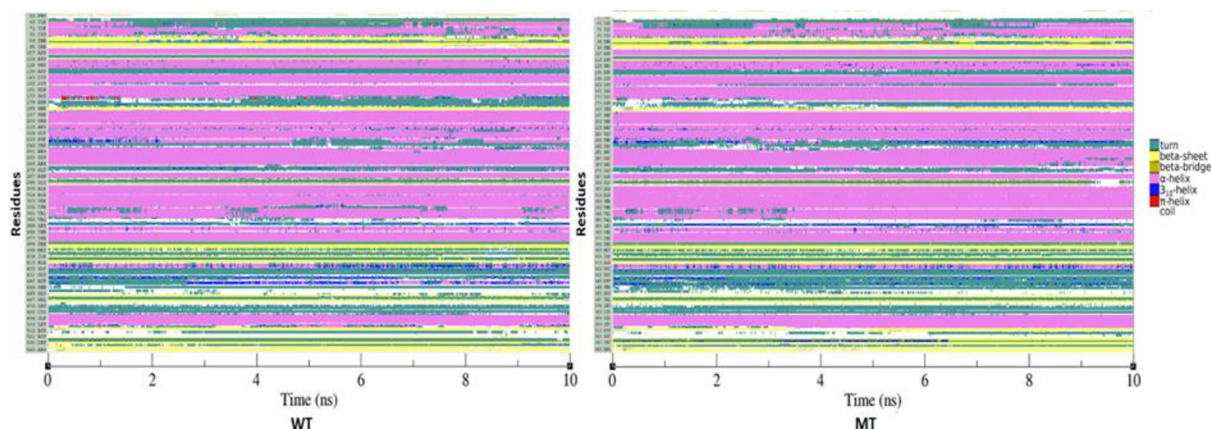


Figure 23 Change in the secondary structure of *CbCyp51* protein of R5 (MT) with comparison S3 (WT) biotype, which is resistant against prochloraz.

4.7.2 Behavioural dynamics of the wild-type and mutant systems

Protein-ligand RMSD values for the wild and the mutant are shown in Figure 24. The root mean square fluctuation (RMSF) versus residue number detected varying fluctuations in almost all the residues in the MT compared to the WT Figure 25. In addition, our results showed that for the *CbCyp51* WT-fungicide interaction, S_{ASA} was ~ 235 nm². However, for the *CbCyp51* MT fungicide interaction, a slight increase in the S_{ASA} (~ 240 nm²), was detected in Figure 26.

Hence, it can be hypothesised that the prochloraz resistance associated with the Y464S mutation may result from an effect on the conformation of the mutant *CbCyp51*.

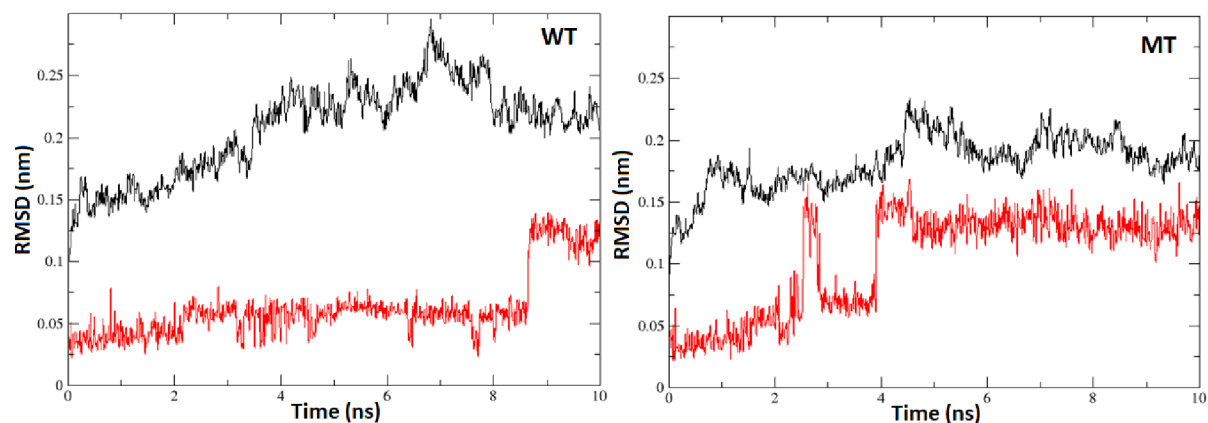


Figure 24 *CbCyp51* protein and prochloraz (ligand) root mean square deviation (RMSD) value of S3 (WT) and R5 (MT) biotype.

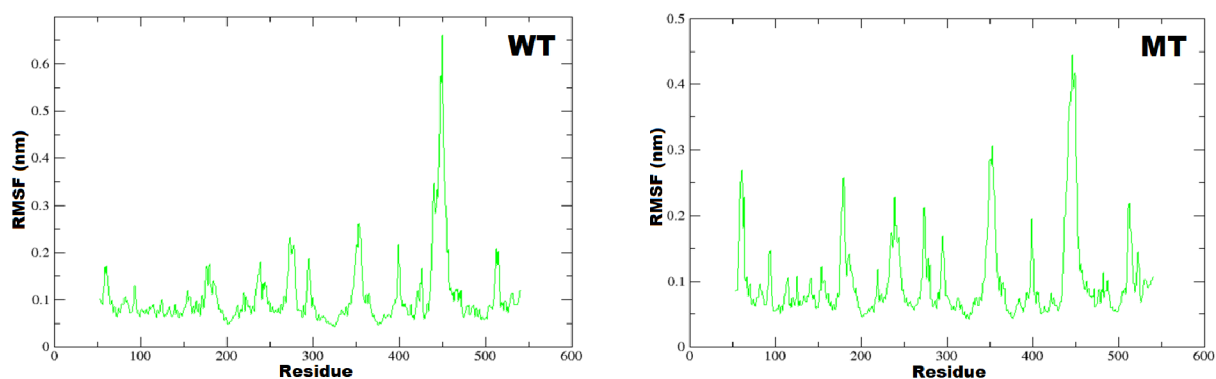


Figure 25 Residue-wise root mean square fluctuation values during prochloraz *CbCyp51* interaction.

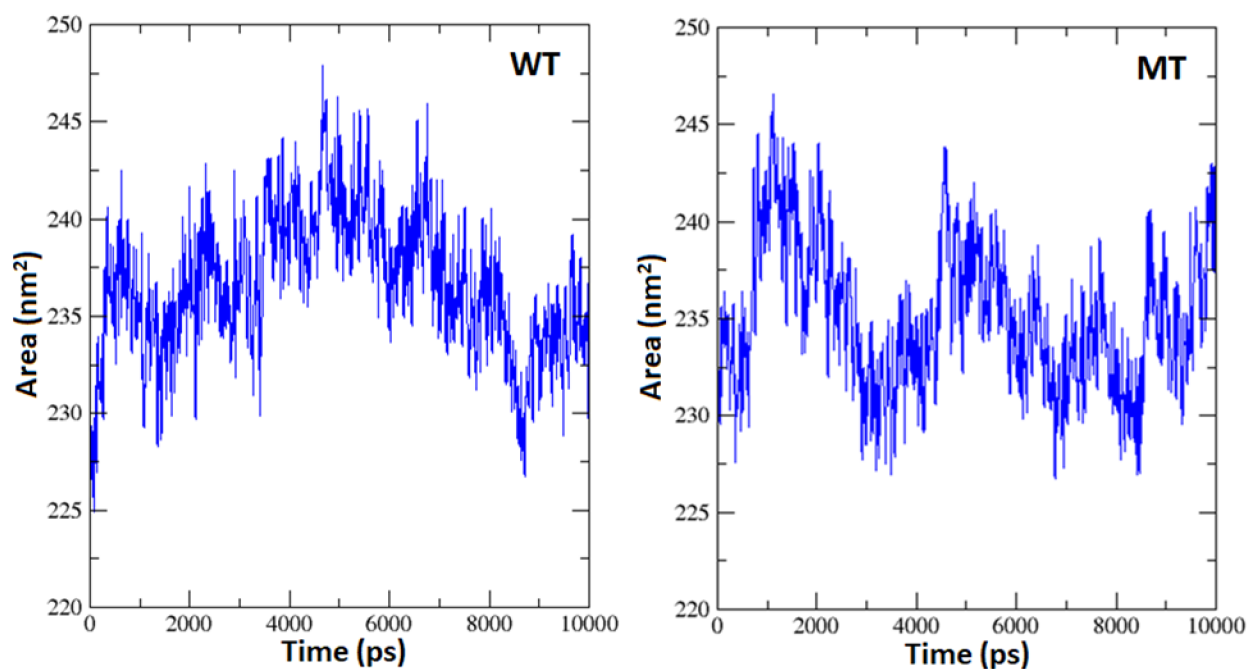


Figure 26 Solvent accessible surface area analysis during prochloraz *CbCyp51* interaction.

4.8 Impact of the Y464S mutation on epoxiconazole binding

4.8.1 Molecular docking studies

The molecular structure of the interaction between epoxiconazole and the wild type (WT) and the mutant (MT) *CbCyp51* is shown in Figure 27. Molecular docking studies revealed that the binding affinity values for the WT and the MT protein were -8.4 kcal/mol and -7.7 kcal/mol, respectively Figure 28. Thirteen amino acids were predicted to be involved in epoxiconazole binding in the case of the *CbCyp51* WT-fungicide interaction. Among these thirteen amino acids, only Ile122A was detected to be involved in hydrogen bonding. However, in the case of the MT *CbCyp51* fungicide interaction, only four amino acids were predicted to be directly involved in epoxiconazole binding. Additionally, no amino acid residue was found to be involved in the MT *CbCyp51* fungicide interaction. Thus, we can predict that hydrogen bonds might play an essential role in fungicide binding. However, this hypothesis requires further validation. Secondary structure analysis showed an increased percentage of alpha helices and random coils in the MT *CbCyp51* fungicide complex compared to the WT *CbCyp51* fungicide complex. Interestingly, we found that the percentage of beta strands also decreased in the MT *CbCyp51* Figure 16. β -strands are known to facilitate hydrogen-bonding interactions during protein-ligand interactions. The decrease in the percentage of the β -strands might explain why no residues are detected in hydrogen bonding in the MT *CbCyp51* fungicide interaction.

Detailed changes in the secondary structure of the *CbCyp51* protein in the presence of ligands for both the WT and MT protein are shown in Figure 29.

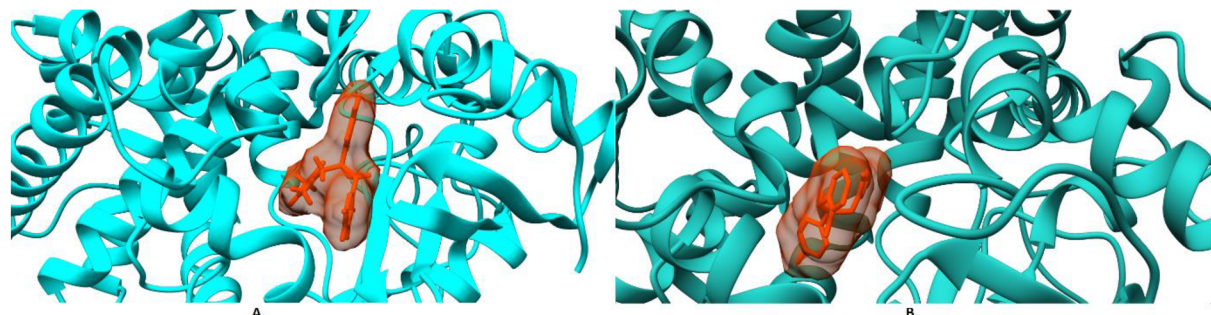


Figure 27 Interaction between epoxiconazole and the *CbCyp51* protein molecular structure of wild type (A.) and the mutant type (B.).

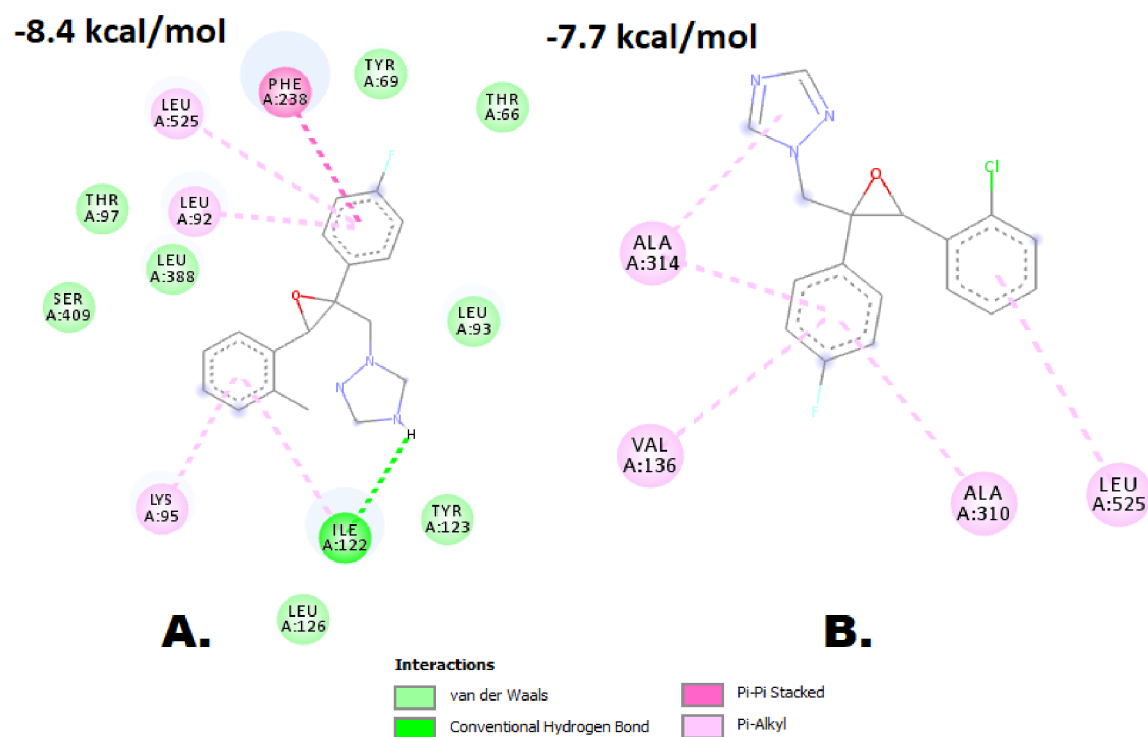


Figure 28 Results for interacting amino acids. A. *CbCyp51* WT and epoxiconazole binding B. *CbCyp51* MT and epoxiconazole binding. The values mentioned in the figures are binding affinity values.

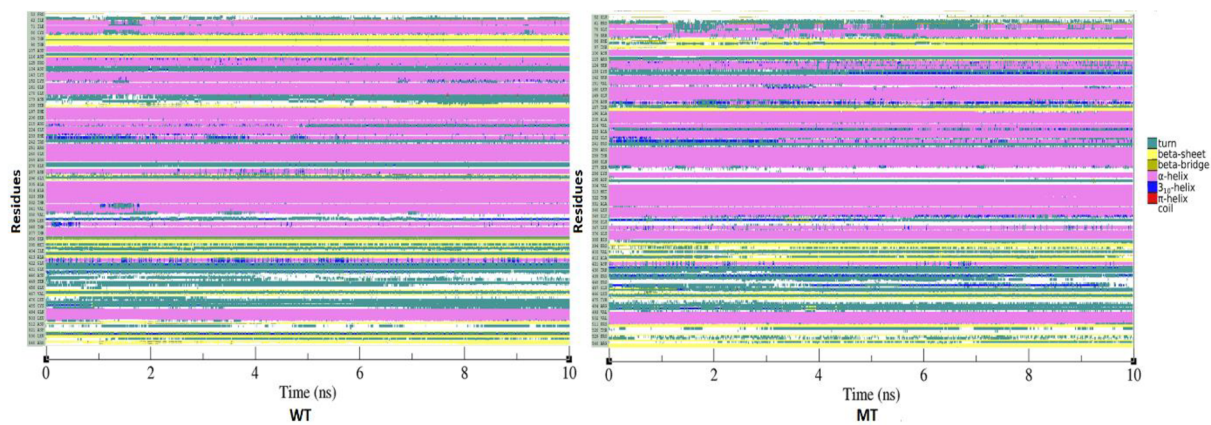


Figure 29 Change in the secondary structure of *CbCyp51* protein of R10 (MT) with comparison S3 (WT) biotype, which is resistant against epoxiconazole.

4.8.2 Behavioural dynamics of the wild-type and mutant-type systems

Protein-ligand RMSD values for the wild-type and the mutant protein are shown in Figure 30. An analysis of root mean square fluctuation (RMSF) versus residue number showed that the amino acid residues from 50 to 250 had slightly higher fluctuations for the MT Protein than WT protein Figure 31. Furthermore, we predicted the SASA for the WT *CbCyp51* fungicide interaction to be $\sim 227.5 \text{ nm}^2$. However, for the MT *CbCyp51* fungicide interaction, the SASA was found to be $\sim 245 \text{ nm}^2$ Figure 32. Hence, we theorise that the epoxiconazole resistance associated with the Y464 mutation may result from an effect on the conformation of the mutant *CbCyp51*.

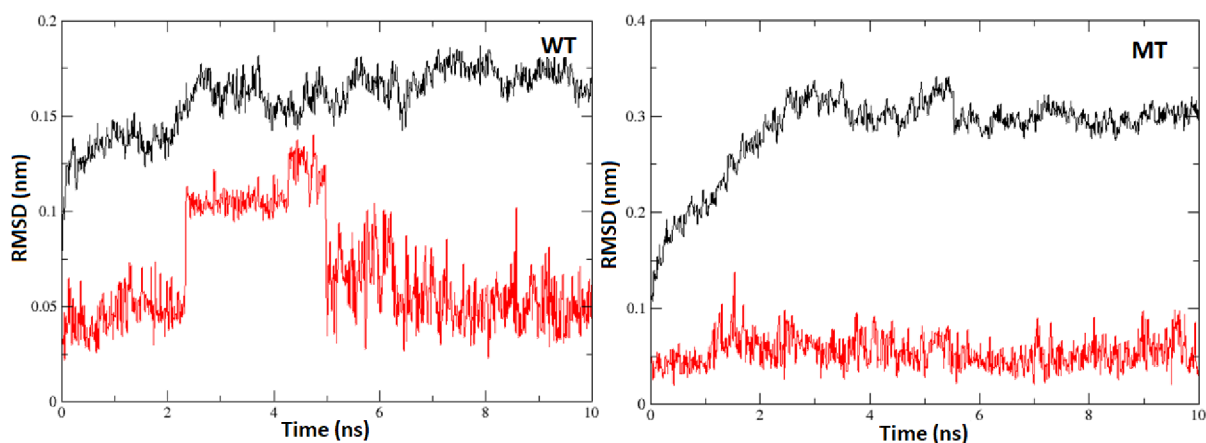


Figure 30 Change in the secondary structure of *CbCyp51* protein of R10 (MT) with comparison S3 (WT) biotype, which is resistant against epoxiconazole.

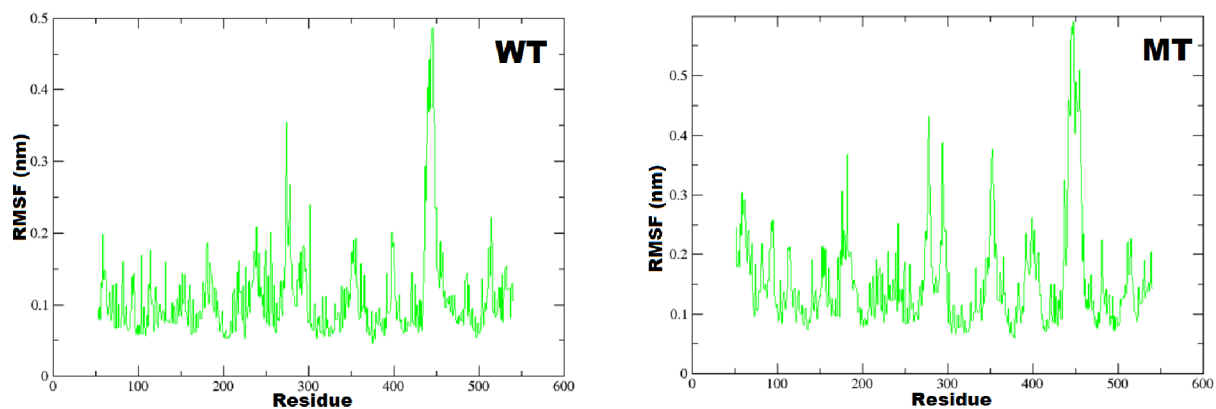


Figure 31 Residue-wise root mean square fluctuation values during epoxiconazole *CbCyp51* interaction.

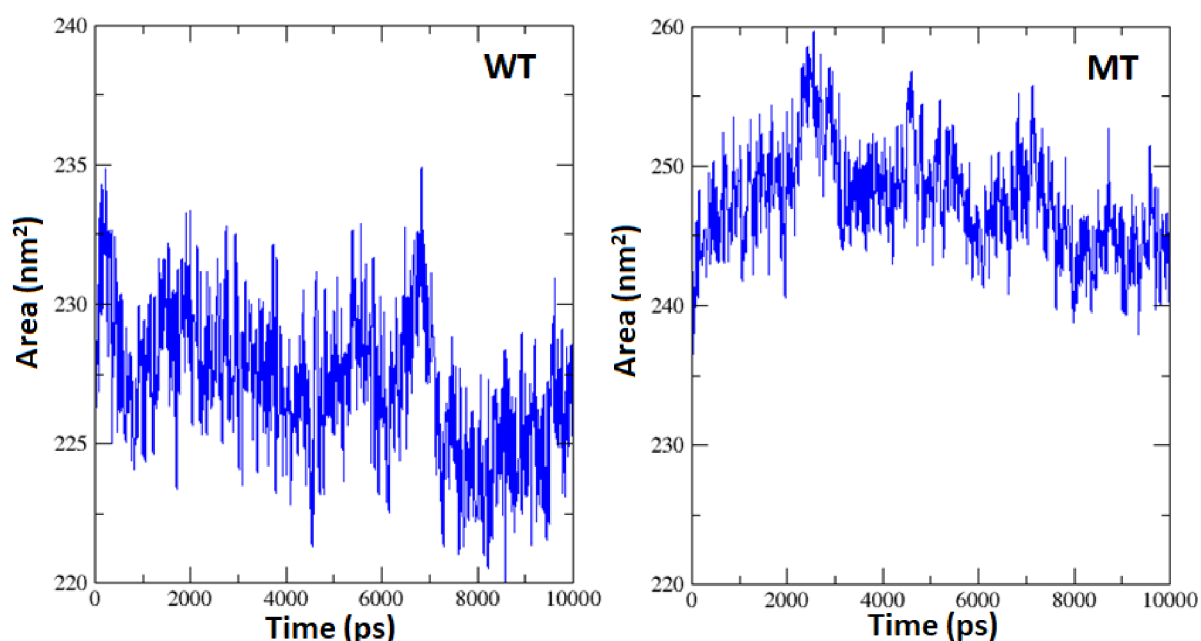


Figure 32 Solvent accessible surface area analysis during epoxiconazole *CbCyp51* interaction.

4.9 RNAseq study analysis

4.9.1 Selection of isolates of *C. beticola* for RNAseq study after exposure to epoxiconazole

Two isolates were used in the transcriptome study collected between 2018-2021 from the Czech Republic sugar beet growing region contrasting for DMI sensitivity. *Cercospora beticola* strain S3 is sensitive to all DMIs fungicides used for the management of CLS exhibiting an EC50 value of $0.006 \mu\text{g mL}^{-1}$ to epoxiconazole, while resistant isolate R8 has an EC50 to epoxiconazole of $61 \mu\text{g mL}^{-1}$.

4.9.2 Quality evaluation of RNAseq Alignments

The genome sequence of *C. beticola* from NCBI was obtained as the reference sequence in the current study. The number of S3 control reads mapping to the genome ranged from 17,062,812 (65.65%) to 17,468,055 (68.31%), while the number of epoxiconazole-treated reads mapping to the *C. beticola* genome ranged from 12,791,966 (62.28%) to 14,711,607 (67.83%).

4.9.3 Predicted Detoxification Genes in CT1 and CB45

Comparative transcriptome profiling showed more differentially expressed genes (DEGs) in *Cercospora beticola*-resistant (Cb-R) than *Cercospora beticola*-sensitive (Cb-S). Functional enrichments identified 15 DEGs in the epoxiconazole-induced Cb-R transcriptome, simultaneously upregulated in *C. beticola* resistance. Figure 33 Venn diagram of DEGs shared in DEG groups RT_vs_RC, RC_vs_SC, RT_vs_ST and RT_vs_RC. The overlapping region comprises the DEGs shared in the four DEG groups Cb-R-I vs Cb-R-NI and RT_vs_RC, RC_vs_SC, RT_vs_ST and RT_vs_ST.

These genes included in the study

- I. ATP-binding cassette (ABC) transporter-encoding genes.
- II. Major Facilitator Superfamily (MFS) transporter-encoding genes.
- III. Ergosterol (ERG) anabolism component genes ERG2, ERG6 and EGR11 (*CBCYP51*).
- IV. Mitogen-activated protein kinase (MAPK) signalling-inducer genes Mkk1 and Hog1.
- V. Ca²⁺/calmodulin-dependent kinase (CaMK) signalling-inducer genes CaMK1 and CaMK2.

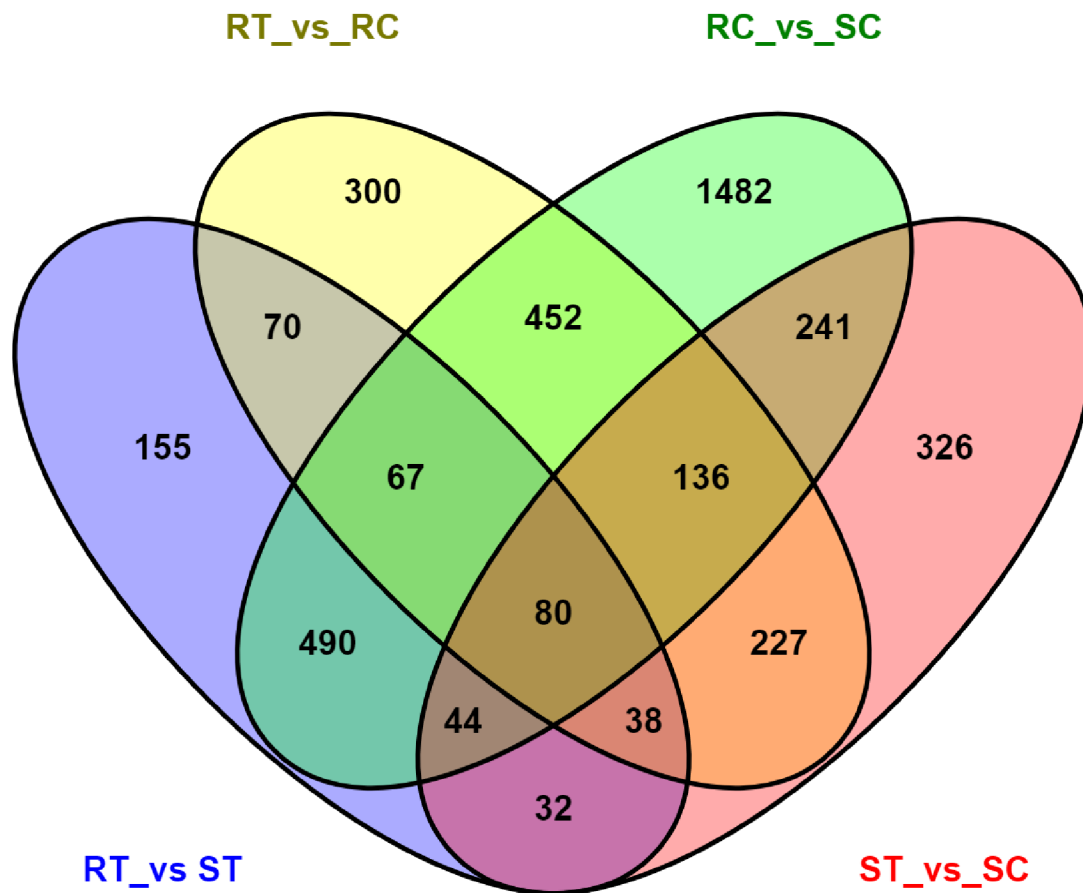


Figure 33 Venn diagram of DEGs shared in DEG groups RT_vs_RC, RC_vs_SC, RT_vs_ST and RT_vs_RC. The overlapping region comprises the DEGs shared in the four DEG groups Cb-R-I vs Cb-R-NI and RT_vs_RC, RC_vs_SC, RT_vs_ST and RT_vs_ST.

4.9.3 Differentially Expressed Genes in epoxiconazole treated and untreated isolates

For gene expression analyses, log₂FC (fold change) values greater than 1 were considered overexpressed, as previously described by [21], while log₂FC values below -1 were considered downregulated. Two hundred fifty-two genes were statistically significantly overexpressed or downregulated in epoxiconazole-treated compared to untreated Figure 33, from which 172 genes were overexpressed and 84 genes downregulated compared to resistance treated and untreated. Whereas 255 genes were overexpressed, and no genes were downregulated compared to resistance and sensitively treated. When comparing resistance treated against sensitive treated, and resistance treated against resistance control and resistance control to sensitive untreated from which, 131 genes were overexpressed, and 16 genes were downregulated. In

addition, comparing each biotype with treated and non-treated, 35 genes are overexpressed, whereas 45 genes are downregulated. Figure 34 differentially expressed genes (DEGs) for results between resistance non-treated vs sensitive non-treated samples. The red dots highlight transcripts of positive and negative values of log₂ Fold Change (logFC), indicating that the sequences were upregulated and downregulated at each time point. The black grey indicates non-differentially expressed genes. Figure 35 distribution of differentially expressed genes (DEGs) for results between resistance-treated and non-treated samples. The red dots highlight transcripts of positive and negative values of log₂ Fold Change (logFC), indicating that the sequences were upregulated and downregulated at each time point. The black grey indicates non-differentially expressed genes. Figure 36 differentially expressed genes (DEGs) for results between resistance-treated and sensitive-treated samples. The red dots highlight transcripts of positive and negative values of log₂ Fold Change (logFC), indicating that the sequences were upregulated and downregulated at each time point. The black grey indicates non-differentially expressed genes. Figure 37 differentially expressed genes (DEGs) for results between sensitive treated vs sensitive non-treated sample. The red dots highlight transcripts of positive and negative values of log₂ Fold Change (logFC), indicating that the sequences were upregulated and downregulated at each time point. The black grey indicates non-differentially expressed genes.

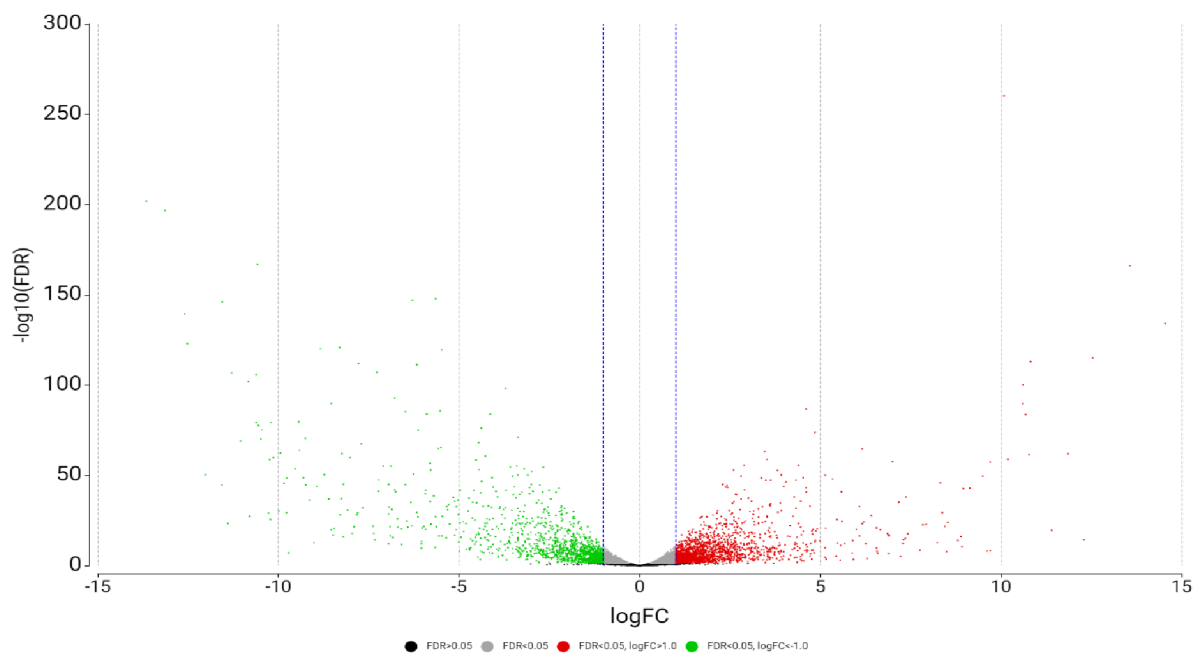


Figure 34 Volcano plot of the distribution of differentially expressed genes (DEGs) for results between resistance non-treated vs sensitive non-treated sample. The red dots highlight transcripts of positive and negative values of log₂ Fold Change (logFC), indicating that the sequences were upregulated and downregulated at each time point. The black grey indicates non-differentially expressed genes.

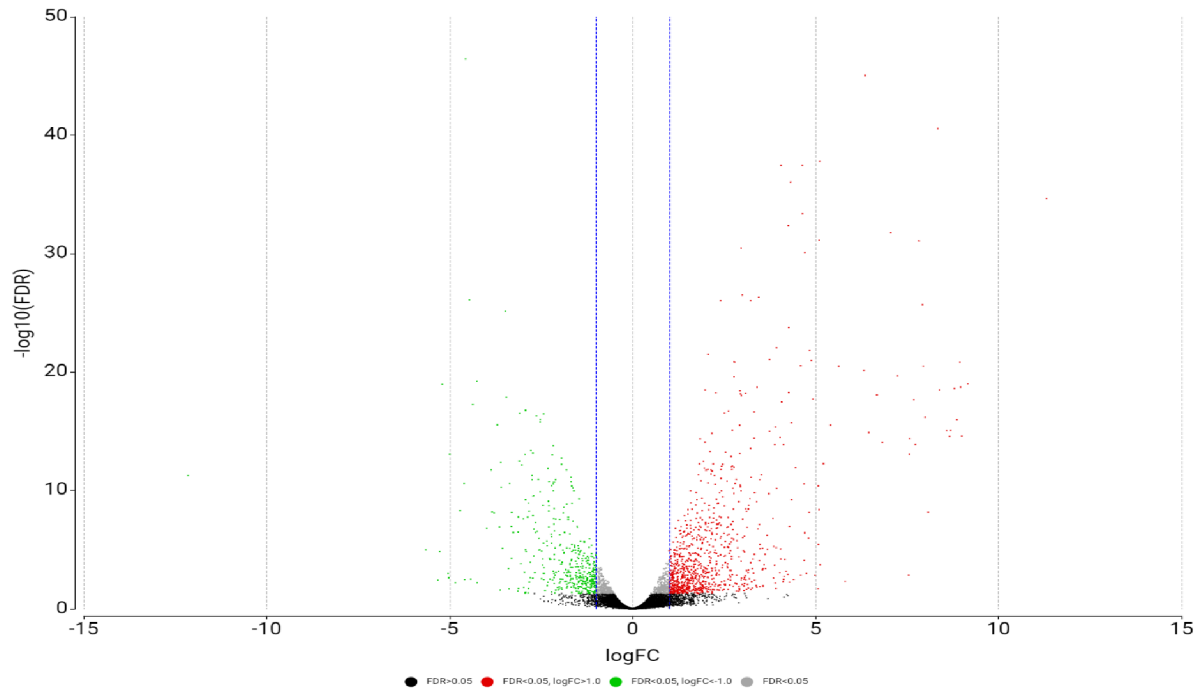


Figure 35 Volcano plot of the distribution of differentially expressed genes (DEGs) for results between resistance-treated and non-treated samples. The red dots highlight transcripts of positive and negative values of log₂ Fold Change (logFC), indicating that the sequences were upregulated and downregulated at each time point. The black grey indicates non-differentially expressed genes.

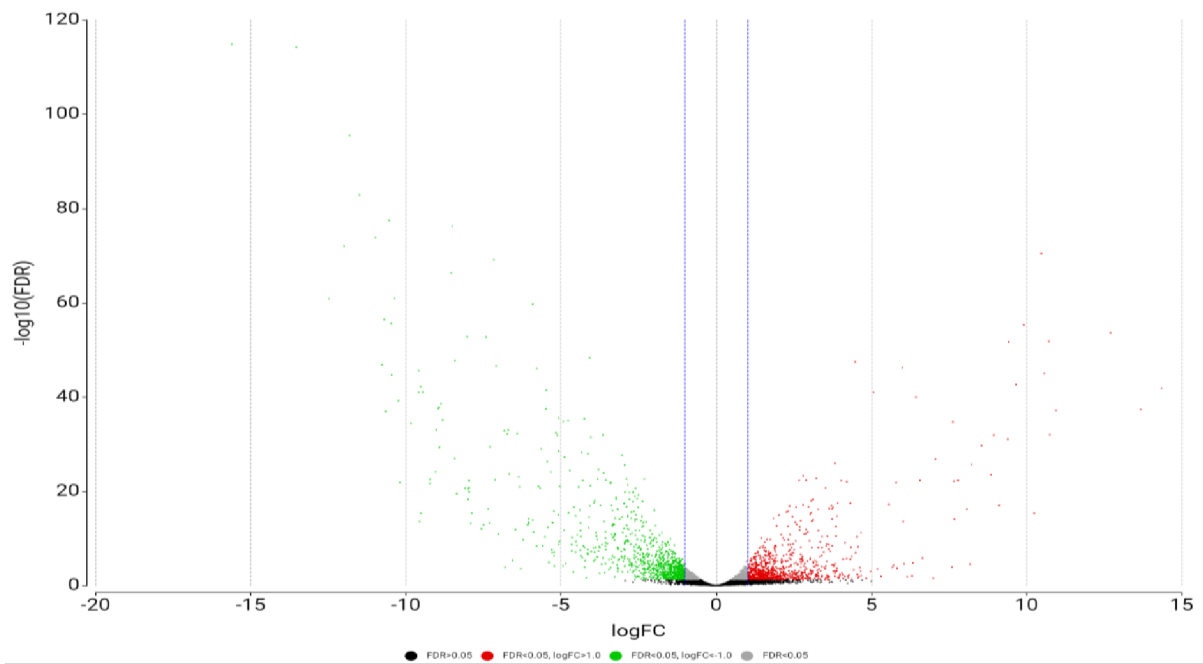


Figure 36 Volcano plot of the distribution of differentially expressed genes (DEGs) for results between the resistance-treated and sensitive-treated samples. The red dots highlight transcripts of positive and negative values of log₂ Fold Change (logFC), indicating that the sequences were upregulated and downregulated at each time point. The black grey indicates non-differentially expressed genes.

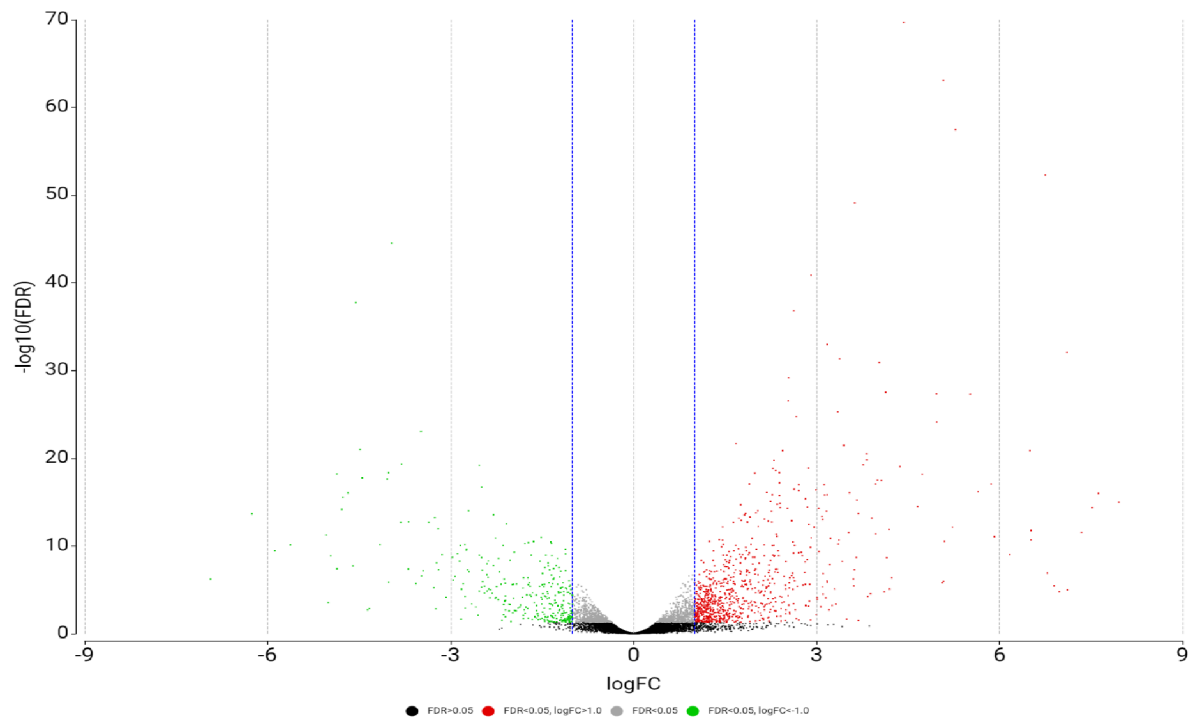


Figure 37 Volcano plot of the distribution of differentially expressed genes (DEGs) for results between sensitive-treated and non-treated samples. The red dots highlight transcripts of positive and negative values of log₂ Fold Change (logFC), indicating that the sequences were upregulated and downregulated at each time point. The black grey indicates non-differentially expressed genes.

Chapter: 5 Discussion

5.1 Importance of CLS disease and its management

Cercospora leaf spot disease is caused by fungus *C. beticola* which continues to be concern for sugar beet cultivation worldwide (Rossi, 1995; Holtschulte, 2000). CLS management programs use to control infections through cultural practices, resistant varieties, and different groups of fungicides (Rossi, 1995; Jacobsen & Franc, 2009). According to FRAC, DMIs have been grouped as medium-risk fungicides for resistance development. Previously, there were multiple resistance mechanisms for DMIs reported including point mutation and overexpression in *CbCyp51* (Bolton *et al.*, 2012, 2016; Zhang *et al.*, 2019, 2021; Kumar *et al.*, 2021; Spanner *et al.*, 2021). These results can improve our understanding of the resistance mechanism of *C. beticola* DMI fungicides.

5.2 *CbCyp51* Gene Mutations in *C. beticola*

Despite the efficiency of these fungicides, the lack of integrated pest management (IPM) strategies has led to resistance problems. Therefore DMI and other fungicides with distinct modes of action should be integrated into IPM programs to reduce fungicide resistance development in phytopathological fungal species globally (Nikou *et al.*, 2009; Bolton *et al.*, 2012; Hawkins *et al.*, 2019; Muellender *et al.*, 2021). In *C. beticola*, mutations within sterol P450 14 α -demethylase (*CbCyp51*), a DMI target enzyme, are reported to associate with decreased sensitivity to DMI fungicides (Shrestha *et al.*, 2020) and other phytopathological fungi e.g., *Rhynchosporium secalis* (Robbertse *et al.*, 2001). During this work, we describe resistance mechanism of DMI fungicides from the Czech Republic (central Europe) in *C. beticola* biotypes. Two hundred and fifty isolates of *C. beticola* were assayed to three DMI fungicides, which identified 6 resistance biotypes R2, R4 R5, R10 contained Y464S, R6 contained I387M, and R11 contained I309T that amino acid exchanges, respectively. Additionally, four sensitive biotypes (S2, S3, S4, and S5) were identified that did not contain *CbCyp51* mutation.

Our results are related to those found by other researchers (Kayamori *et al.*, 2021). Our data should be studied in future monitoring surveys since they also occur in conserved regions of *CbCyp51* gene (Muellender *et al.*, 2021). Moreover, these mutations occurred in conserved domains of the *CbCyp51* sequence of other phytopathogenic fungi, suggesting that these regions are important for the formation of binding pockets for the fungicide (Muellender *et al.*, 2021). The mutation Y464S is equivalent to the Y461S amino acid exchange in the closely related fungus *Z. tritici* (Trkulja *et al.*, 2017; Huf *et al.*, 2018) and I309T was found near the substrate recognition site 2 near the positions 309–118 of *Z. tritici* (Lepesheva & Waterman,

2007; Brunner *et al.*, 2008; Tyndall *et al.*, 2016; Huf *et al.*, 2018; Zhang *et al.*, 2019). It is probable that the mutations hinder the access of DMIs to the active site of the protein. As shown for *Z. tritici*, unlike single nucleotide polymorphism was associated with changing levels of sensitivity decreased towards different DMI (Cools *et al.*, 2011; Heick *et al.*, 2017).

5.3 *CbCyp51* Gene Expression Analysis

A fungicide induced upregulation of *CbCyp51* had been shown in all three biotypes displaying high EC₅₀ values. The fungicide induction of the gene expression follows a positive relationship where strains with higher EC₅₀ values tend to have high expression of *CbCyp51*. The absence of the ergosterol end product activates *CbCyp51* induction (Muellender *et al.*, 2021). Such an upregulation of *CbCyp51* was already observed e.g. in *C. beticola* and other phytopathogenic fungi *Pyrenophora teres* or *Fusarium graminearum* but a stronger induction in more sensitive isolates was not reported before (Fan *et al.*, 2013; Mair *et al.*, 2016; Muellender *et al.*, 2021).

5.4 Impact of the Mutations on Fungicide Binding

For better understanding of fungicide resistance mechanism of DMI fungicides, it is important to study the interaction between the fungicide and the target protein *CbCyp51*. With the change in the conformity of the binding pocket, the drug might become less effective, thus developing resistance (Zhou *et al.*, 2015). In this PhD work, we explored molecular docking of *CbCyp51* protein for three mutations in *C. beticola* varies among R biotypes (R2, R4, R5, R6, R10, and R11) to three DMI fungicides and demonstrated molecular docking models. Our analysis suggested that mutations Y464S, I387M and I309T in the *CbCyp51* resistant strains were binding affinity increased compared with sensitive strains (Cao *et al.*, 2017; Wei *et al.*, 2020). Molecular docking experiment shows that Y464S, I387M and I309T changes the conformation of the *CbCyp51* genotype with DMIs fungicides, which is one of the molecular mechanisms of resistance development (Wei *et al.*, 2020). Overall, twelve amino acid residues were predicted to be involved in binding and no amino acid residues were involved in hydrogen bonding with WT-fungicide interaction with prochloraz. However, for mutated *CbCyp51*-fungicide interactions, only six amino acids directly involved in binding whereas one hydrogen bond was found to be involved with prochloraz, suggesting these amino acid residues might be important for prochloraz binding. Overall, six amino acid residues were predicted to be directly involved in propiconazole binding in the *CbCyp51* WT-fungicide and *CbCyp51* MT-fungicide interaction were predicted to be directly involved in propiconazole binding. One amino acid residue was found to be involved in hydrogen bonding in either case. Moreover, our analysis

detected six interacting amino acid residues (Leu126, Tyr137, Phe233, Ile384, Ile387, and Lue525) involved in the WT. Whereas in *CbCyp51*-MT interaction amino acid residues (Lys149, Lys152, Met450, Ser464, Gly465, and Lue466). Overall, seven amino acid residues were predicted to be directly involved in epoxiconazole binding in the case of the *CbCyp51* WT-fungicide interaction. Among these 7 amino acids residues, only Tyr137, Lys148 and His483 were detected to be involved in hydrogen bonding. However, in the case of the MT *CbCyp51* fungicide interaction, only ten amino acid residues were predicted to be directly involved in epoxiconazole binding. Additionally, one (Gly315) amino acid residue was found to be involved in hydrogen bonding the MT *CbCyp51* fungicide interaction. Thus, we can predict that hydrogen bonds might have an essential role in epoxiconazole binding. Hydrogen bonds are known to provide most of the directional interactions that involves molecular recognition (Hubbard & Haider, 2010). In this study molecular docking with the homology-modelled of proteins with existing fungicides can serve as an important prototype. Previously structural rationale study was conducted for triazole, and imidazole resistance associated with *CbCyp51* mutations (Parker *et al.*, 2014). In previous studies, modelled the WT and MT of *CbCyp51* gene from *Mycosphaerella graminicola* and another study had also conducted on *Colletotrichum truncatum* for DMI fungicides (Mullins *et al.*, 2011; Chen *et al.*, 2018). The same phenomenon was also found for four amino acid alterations (L208Y, H238R, S302A, and I366L) in *CbCyp51A*- DMI fungicide binding in *C. truncatum* (Chen *et al.*, 2018). Their results suggested that four alterations associated with reduce azole affinity (Mullins *et al.*, 2011; Chen *et al.*, 2018). Although, these hypotheses require further validation. Few studies have utilized in silico techniques to address fungicide resistance mechanisms. Hence, the previous studies along with our current study will provide prospective for an in-silico screening system and reliable predictive approach to evaluate the probability of variants exhibiting fungicides resistance. These studies will open many potential opportunities leading to the discovery of new fungicidal property compounds.

5.5 RNAseq study analysis

Insight into the molecular basis of epoxiconazole resistance might lead to molecular techniques to identify DMI-resistant isolate for fungicide resistance management programs. In this study, we profiled the response of two *C. beticola* isolates contrasting for resistance to the critical DMI fungicide epoxiconazole. Although our initial concern was to identify induced genes in the DMI-resistant isolates, we observed a significant overlap of genes differentially expressed in both isolates suggesting a common background response when exposed to epoxiconazole. The clear induction of ergosterol pathway genes indicates maintenance or reinforcement of cell

membrane integrity is a common response when exposed to epoxiconazole. Similarly, a isolates of *Aspergillus niger* responded to the ergosterol-targeting fungicide fenpropimorph with enhanced expression of various ergosterol pathway genes identified utilizing an Affymetrix microarray (Meyer *et al.*, 2007). Cools *et al.* (2007) used a cDNA microarray method to identify three induced genes in an epoxiconazole-sensitive isolates of *Z. tritici*, all of which were ergosterol biosynthesis pathway genes (Erg5, Erg24, and Erg25). These same genes were caused in the *Z. tritici* epoxiconazole-resistant isolates but with lesser transcript levels (Cools *et al.*, 2007). In the human pathogen *Candida albicans*, induced expression of *CbCyp51* and other genes engaged with ergosterol biosynthesis is related with DMI exposure (De Backer *et al.*, 2001; Liu *et al.*, 2005; Dunkel *et al.*, 2008). Although the majority ergosterol biosynthesis genes were induced to like levels in our study, *CbCyp51* was induced to much higher levels in the DMI-resistant isolates compared to the sensitive isolates, underlying a key difference between sensitive and resistant *C. beticola* isolates and supporting our prior results that showed native *CbCyp51* expression is generally higher. Expression is inducible in DMI-resistant field isolates (Kumar *et al.*, 2021).

The mechanism for the upregulation of *CbCyp51* and/or other ergosterol biosynthesis genes is currently unknown in *C. beticola*. In the human pathogen *Candida albicans*, the zinc cluster transcription factor Upc2p has been indicated to regulate the expression of *CbCyp51* and other genes engaged in ergosterol biosynthesis upon exposure to DMIs (MacPherson *et al.*, 2005). This work identified several transcription factors induced in response to epoxiconazole. It will be interesting to investigate therefore these transcription factors regulate the expression of ergosterol biosynthesis genes in *C. beticola*. Like to DMI exposure, cellular oxygen deficiency has been indicated to induce ergosterol biosynthesis genes. For example, several ergosterol biosynthesis genes were up-regulated in the rice blast disease fungus *Magnaporthe oryzae* in response to hypoxia (Choi *et al.*, 2015). Another case of fungal response to hypoxia is the induction of the sterol regulatory binding protein (SREBP) pathway, which causes ergosterol biosynthesis and hyphal increase to scavenge more oxygen in human fungal pathogens (Hughes *et al.*, 2005). SREBPs are transcription factors that are activated when sterols are depleted due to triggers such as hypoxia and iron limitation (Blatzer *et al.*, 2011). Active such as hypoxia and iron limitation (Blatzer *et al.*, 2011). Active SREBP goes on the expression of sterol synthesis protein and additional oxygen-dependent proteins (Blatzer *et al.*, 2011; Choi *et al.*, 2015). Lately, Liu *et al.* (2015) identified a novel SREBP gene that was required for DMI resistance and *CbCyp51* over-expression in *Penicillium digitatum*. Our results also identified a

gene encoding SREBP induced alongside ergosterol biosynthesis genes in both isolates, perhaps suggesting that oxygen is limiting and/or ergosterol deficiency is sensed in *C. beticola* cells upon DMI exposure. Hypoxia and heme deficiency are also well-known to induce RTA1 expression (Protchenko *et al.*, 2008), which was the highly-induced gene in the DMI-resistant strain in our study. The RTA1 gene was originally found during a screen for genes that confer resistance to the sterol biosynthesis inhibitor 7-amino cholesterol in *S. cerevisiae* (Soustre *et al.*, 1996). RTA1 proteins encode a protein with seven transmembrane spans (Manente & Ghislain, 2009). Recent evidence indicates several gene networks involved with diverse cellular responses, including hypoxia, reactions to some cytotoxic drugs, and ergosterol biosynthesis converge on the RTA1 gene (Kolaczowska *et al.*, 2012), suggesting that RTA1 is involved with the response to various stresses by fortifying the cell membrane.

In addition, to characterize this phenomenon, it may suggest that *C. beticola* responds to protoplast development in the transformation of a new cell wall that is particularly fortified, which results in enhanced DMI resistance. Likewise, the cell membrane might be modified due to PEG exposure, resulting in increased DMI resistance. To our knowledge, this trend has not been described in filamentous fungi. Since there are no other reported transformation alternatives for *C. beticola*, future research aimed towards developing an *Agrobacterium tumefaciens*-based transformation procedure will be necessary to characterize genes linked with DMI resistance in this pathogen.

Chapter: 6 Conclusion

We identified twelve different *C. beticola* *CbCyp51* strains correlating with highly reduced sensitivity towards DMI fungicides (propiconazole, prochloraz and epoxiconazole). Mutations I387M, I309T, and Y464S were found only singularly but should be monitored in the future. The most frequent mutations were Y464S. These SNPs were found to occur in highly conserved domains of the target protein *CBCYP51*, not only in *C. beticola* but also other phytopathogenic fungi displaying reduced DMI sensitivity.

Our expectations and previous studies with *C. beticola* found a stronger fungicide-induced over-expression of *CbCyp51* in isolates with very low EC50 values compared to high EC50 strains. We have also found significant differences in relative gene copy number variation in the three resistance strains, one from each DMI and relative gene overexpression in six

resistance strains, each two from propiconazole, prochloraz and epoxiconazole. One strain from each DMI did not find relative gene copy number variation nor relative gene overexpression.

Further experiments with reverse genetic, transcriptomics and proteomics systems are required to illuminate the role of the target site mutations and gene copy number on the expression level of *CbCyp51* and the DMIs resistance in *C. beticola*.

Chapter: 7 Publication

1. Characterization of the molecular mechanisms of resistance against DMI fungicides in *Cercospora beticola* populations from the Czech Republic.
2. Systematic Identification of Suitable Reference Genes for Quantitative Real-Time PCR Analysis in *Melissa officinalis L.*
3. Evaluation of the Ability of Seven Active Ingredients of Fungicides to Suppress *Phytophthora cactorum* at Diverse Life Stages, and Variability in Resistance Found among Isolates.
4. Identification of the most suitable reference genes for nanoparticle stress response in *Salvia rosmarinus* (rosemary) produced under in vitro conditions.
5. Socio-Economic Status of Farmers in Raisen District of Madhya Pradesh: A Case Study

LIST OF TABLES

Table 1 Taxonomy of <i>Cercospora beticola</i> in ascending order	13
Table 2 Biological control agent for plant diseases	14
Table 3 List of primers used in this study. Primer pairs RT_F1-RT_R1 and RT_F2-RT_R2 were used in both copy number variation as well as gene expression analysis. Primer pairs F1-R1 and F2-R2 and cloning_F1- cloning_R1 and cloning_F2- cloning_R2 were used to isolate and clone partial <i>CbCyp51</i> gene from <i>C. beticola</i>	20
Table 4 Fungicide sensitivity assays. Top 20 sensitive and resistance isolates of <i>C. beticola</i> out 250 which was screened against 3 DMIs fungicides e.g. propiconazole, prochloraz and epoxiconazole. EC50 value were calculated using graph pad prism software(9.0.0), based on mean colony diameter and radial growth of each isolate and all EC50 values are in µg/ml. ..	22
Table 5 Effective concentration at 50% (EC50) for <i>C.beticola</i> isolates collected from 2018-20. Fungicide sensitivity assay against two fifty isolates performed and from screening, four highly resistance and two sensitive isolate for each fungicide.....	22
Table 6 Resistance factor against S2 of all resistance biotype for all three DMIs fungicides .	23
Table 7 Resistance factor against S3 of all resistance biotype for all three DMIs fungicides .	23

Table 8 Result of *CbCyp51* mutation amino acid change in *CbCyp51* in comparison with wild type and isolate CVA41 from NCBI (GenBank Acc. No. KU665583.1). 25

LIST OF FIGURES

Figure 1 The top 10 sugar beet producing countries from 1994-2018 (FAO 2018). 9

Figure 2 Production /Yield quantities of sugar beet around the globe since 1994-2018 (FAO, 2018). 9

Figure 3 The sugar beet production in each continent since 1995-2018 (FAO, 2018). 9

Figure 4 Symptoms of *C. beticola* leaf spot on a leaf of sugar beet field in leaf in the left side and CLS infected sugar beet field in the right side. 11

Figure 5 Cercospora leaf spot (CLS) disease cycle in sugar beet. Disease infection is initiated by airborne and/or splash dispersed conidia that permeate the sugar beet leaf via stomata and provide growth to intercellular hyphal development. CLS spot form on the leaves after the switch to necrotrophy, which develops symptoms within 7 days. Pseudostromata developed in the lesion, and *C. beticola* asexually produce spores, leading to multiple infection cycles in one growing season. The Pseudostromata can also survive overwinter in plant debris at the end of the season (Image source)(Rangel et al., 2020b). 15

Figure 6 Total RNA integrity of all *C. beticola* isolates Cb-Resistance and Cb-Sensitive tested in agarose gel before samples sending for transcriptome sequencing. 26

Figure 7 Artificial inoculation of *C. beticola* in susceptible cultivar of sugar beet at various time after inoculation in growth chamber and leaf spots symptoms counted on per leaf on DAI. .. 33

Figure 8 Analysis of relative gene expression. The relative gene expression values are in terms of $2^{-\Delta\Delta Ct}$ values. (A) Relative gene expression level between the treated and non-treated of S3 and resistance strain with propiconazole and DMSO. (B)Relative gene expression level between the treated and non-treated of S4 and resistance strain with prochloraz and DMSO. (C) Relative gene expression level between the treated and non-treated of S3 and resistance strain with epoxiconazole and DMSO. 35

Figure 9 Analysis of copy number variation. The relative copy number values are in terms of $2^{-\Delta\Delta Ct}$ values. “*” denotes significant at 5% significant level. (A) Copy number variation in difference between S3 and R2 at the 5% significant level. (B) Copy number variation in difference in only R4 compared with S2 and however R6 and R11 was not found any significant difference at the 5% significance level.	36
Figure 10 Structure validation parameter Ramachandran plot of Sensitive biotype S2 and S3 without any mutation.....	37
Figure 11 Structure validation parameter Ramachandran plot of resistance biotype with mutation Y464S.....	38
Figure 12 Structure validation parameter Ramachandran plot of resistance biotype with mutation I387M.....	39
Figure 13 Structure validation parameter Ramachandran plot of resistance biotype with mutation I309T.....	40
Figure 14 Interaction between propiconazole and the <i>CbCyp51</i> protein molecular structure of wild type (A.) and the mutant type (B.).	41
Figure 15 Results for interacting amino acids. (A) <i>Cb_CbCyp51_WT</i> and propiconazole binding, (B) <i>CbCyp51</i> MT and propiconazole binding. The mentioned values in the figures are binding affinity values.....	42
Figure 16 Results for secondary structure analysis during protein-ligand interaction.....	42
Figure 17 Change in secondary structure of <i>CbCyp51</i> protein of R2 (MT) with comparison S3 (WT) biotype, which is resistance to propiconazole.....	43
Figure 18 <i>CbCyp51</i> protein and propiconazole (ligand) Root mean square deviation (RMSD) value of S3 (WT) and R2 (MT) biotype.....	44
Figure 19 Residue wise root mean square fluctuation values during propiconazole <i>CbCyp51</i> interaction.....	44

Figure 20 Solvent accessible surface area analysis during propiconazole <i>CbCyp51</i> interaction.....	44
Figure 21 Interaction between prochloraz and the <i>CbCyp51</i> protein molecular structure of wild type (A) and the mutant type (B).....	45
Figure 22 Results for interacting amino acids. A. <i>CbCyp51</i> WT and prochloraz binding (B) <i>CbCyp51</i> MT and prochloraz binding. The mentioned values in the figures are binding affinity values.....	46
Figure 23 Change in secondary structure of <i>CbCyp51</i> protein of R5 (MT) with comparison S3 (WT) biotype, which is resistance against prochloraz.	46
Figure 24 <i>CbCyp51</i> protein and prochloraz (ligand) Root mean square deviation (RMSD) value of S3 (WT) and R5 (MT) biotype.....	47
Figure 25 Residue wise root mean square fluctuation values during prochloraz <i>CbCyp51</i> interaction.....	47
Figure 26 Solvent accessible surface area analysis during prochloraz <i>CbCyp51</i> interaction.....	48
Figure 27 Interaction between epoxiconazole, and the <i>CbCyp51</i> protein molecular structure of wild type (A.) and the mutant type (B.).....	49
Figure 28 Results for interacting amino acids. A. <i>CbCyp51</i> WT and epoxiconazole binding B. <i>CbCyp51</i> MT and epoxiconazole binding. The values mentioned in the figures are binding affinity values.....	49
Figure 29 Change in secondary structure of <i>CbCyp51</i> protein of R10 (MT) with comparison S3 (WT) biotype, which is resistance against epoxiconazole.....	50
Figure 30 Change in secondary structure of <i>CbCyp51</i> protein of R10 (MT) with comparison S3 (WT) biotype, which is resistance against epoxiconazole.....	50
Figure 31 Residue wise root mean square fluctuation values during epoxiconazole <i>CbCyp51</i> interaction.....	51
Figure 32 Solvent accessible surface area analysis during epoxiconazole <i>CbCyp51</i> interaction.....	51

Figure 33 Venn diagram of DEGs shared in DEG groups RT_vs_RC, RC_vs_SC, RT_vs_ST and RT_vs_RC. The overlapping region comprises the DEGs shared in the four DEG groups Pi-R-I vs Pi-R-NI and RT_vs_RC, RC_vs_SC, RT_vs_ST and RT_vs_ST. 53

Figure 34 Volcano plot of distribution of differentially expressed genes (DEGs) for results between resistance non treated vs sensitive non treated sample. The red dots highlight transcripts of positive and negative values of log₂ Fold Change (logFC), indicating that the sequences were upregulated and downregulated at each time point. The black grey indicates non-differentially expressed genes. 54

Figure 35 Volcano plot of distribution of differentially expressed genes (DEGs) for results between resistance treated vs resistance non treated sample. The red dots highlight transcripts of positive and negative values of log₂ Fold Change (logFC), indicating that the sequences were upregulated and downregulated at each time point. The black grey indicates non-differentially expressed genes. 55

Figure 36 Volcano plot of distribution of differentially expressed genes (DEGs) for results between resistance treated vs sensitive treated sample. The red dots highlight transcripts of positive and negative values of log₂ Fold Change (logFC), indicating that the sequences were upregulated and downregulated at each time point. The black grey indicates non-differentially expressed genes. 55

Figure 37 Volcano plot of distribution of differentially expressed genes (DEGs) for results between sensitive treated vs sensitive non treated sample. The red dots highlight transcripts of positive and negative values of log₂ Fold Change (logFC), indicating that the sequences were upregulated and downregulated at each time point. The black grey indicates non-differentially expressed genes. 56

LIST OF ABBREVIATIONS

AA	Amino acid
ABC	ATP-binding cassette
ANOVA	Analysis of variance
bp	Base pair
cDNA	Complementary DNA
cDNA-AFLP	cDNA-amplified fragment length polymorphism
CFP	Cercosporin facilitator protein

CM Complete medium

CLS Cercospora leaf spot disease

DAP Days after planting

DMIs demethylation inhibitors

DNA Deoxyribonucleic acid

dpi Days post inoculation

dsRNA Double stranded RNA

DSS Disease severity scores

Ecp Extracellular protein

EC Effective concentration

FCR Fusarium crown rot

GUS β -glucuronidase

ITS Internal transcribed spacer

kb Kilo base

miRNA Micro RNA

MM Minimal medium

MP-PCR Microsatellite-primed PCR

NCBI National Centre for Biotechnology Information

MT Mutated type

NL Nonlinear

nt Nucleotide

NTC No-template control

ORF Open reading frame

PCR Polymerase chain reaction

PDA Potato dextrose agar

PDB Potato dextrose broth

qPCR Quantitative polymerase chain reaction

RAPD Random amplified polymorphic DNA

RH Relative humidity

RNA Ribonucleic acid

rRNA Ribosomal RNA

RF resistance factor

RT Room temperature

RT-PCR Reverse transcription-polymerase chain reaction

WT Wild type

LITERATURE CITED

- Alexander BJR, Stewart A, 2001. Glasshouse screening for biological control agents of *Phytophthora cactorum* on apple (*Malus domestica*). *New Zealand journal of crop and horticultural science* **29**, 159–169.
- Amir M, Mohammad T, Kumar V *et al.*, 2019. Structural Analysis and Conformational Dynamics of STN1 Gene Mutations Involved in Coat Plus Syndrome. *Frontiers in Molecular Biosciences* **6**.
- Andrews S, 2010. FastQC: a quality control tool for high throughput sequence data.
- Blatzer M, Barker BM, Willger SD *et al.*, 2011. SREBP Coordinates Iron and Ergosterol Homeostasis to Mediate Triazole Drug and Hypoxia Responses in the Human Fungal Pathogen *Aspergillus fumigatus*. *PLOS Genetics* **7**, e1002374.
- Bolton MD, Birla K, Rivera-Varas V, Rudolph KD, Secor GA, 2011. Characterization of CbCyp51 from Field Isolates of *Cercospora beticola*. *Phytopathology*® **102**, 298–305.
- Bolton MD, Birla K, Rivera-Varas V, Rudolph KD, Secor GA, 2012. Characterization of CbCyp51 from field isolates of *Cercospora beticola*. *Phytopathology* **102**, 298–305.
- Bolton MD, Ebert MK, Faino L *et al.*, 2016. RNA-sequencing of *Cercospora beticola* DMI-sensitive and-resistant isolates after treatment with tetraconazole identifies common and contrasting pathway induction. *Fungal Genetics and Biology* **92**, 1–13.
- Bolton MD, Rivera V, Secor G, 2013. Identification of the G143A mutation associated with QoI resistance in *Cercospora beticola* field isolates from Michigan, United States. *Pest Management Science* **69**, 35–39.
- Brent KJ, Hollomon DW, 1995. *Fungicide resistance in crop pathogens: how can it be managed?* GIFAP Brussels.
- Brunner PC, Stefanato FL, McDonald BA, 2008. Evolution of the CYP51 gene in *Mycosphaerella graminicola*: evidence for intragenic recombination and selective replacement. *Molecular plant pathology* **9**, 305–316.
- Büttner G, Pfähler B, Petersen J, 2003. Rhizoctonia root rot in Europe—incidence, economic importance and concept for integrated control. In: *Proceedings of the 1st joint IIRB-ASSBT Congress, San Antonio*. 897–901.

- Cao M-J, Zhang Y-L, Liu X *et al.*, 2017. Combining chemical and genetic approaches to increase drought resistance in plants. *Nature communications* **8**, 1–12.
- Chen S, Wang Y, Schnabel G *et al.*, 2018. Inherent Resistance to 14 α -Demethylation Inhibitor Fungicides in *Colletotrichum truncatum* Is Likely Linked to CYP51A and/or CYP51B Gene Variants. *Phytopathology*® **108**, 1263–1275.
- Choi J, Chung H, Lee G-W, Koh S-K, Chae S-K, Lee Y-H, 2015. Genome-wide analysis of hypoxia-responsive genes in the rice blast fungus, *Magnaporthe oryzae*. *PloS one* **10**, e0134939.
- Chupp CC, 1953. A monograph of the fungus genus *Cercospora*. *A Monograph of the fungus genus Cercospora*.
- Cools HJ, Fraaije BA, Bean TP, Antoniw J, Lucas JA, 2007. Transcriptome profiling of the response of *Mycosphaerella graminicola* isolates to an azole fungicide using cDNA microarrays. *Molecular Plant Pathology* **8**, 639–651.
- Cools HJ, Mullins JGL, Fraaije BA *et al.*, 2011. Impact of Recently Emerged Sterol 14 α -Demethylase (CYP51) Variants of *Mycosphaerella graminicola* on Azole Fungicide Sensitivity. *Applied and Environmental Microbiology* **77**, 3830–3837.
- De Backer MD, Ilyina T, Ma X-J, Vandoninck S, Luyten WH, Vanden Bossche H, 2001. Genomic profiling of the response of *Candida albicans* to itraconazole treatment using a DNA microarray. *Antimicrobial agents and chemotherapy* **45**, 1660–1670.
- Dekker J, 1982. Countermeasures for avoiding fungicide resistance. *Fungicide resistance in crop protection*, 177–186.
- Dobin A, Davis CA, Schlesinger F *et al.*, 2013. STAR: ultrafast universal RNA-seq aligner. *Bioinformatics* **29**, 15–21.
- Dunkel N, Liu TT, Barker KS, Homayouni R, Morschhäuser J, Rogers PD, 2008. A gain-of-function mutation in the transcription factor Upc2p causes upregulation of ergosterol biosynthesis genes and increased fluconazole resistance in a clinical *Candida albicans* isolate. *Eukaryotic cell* **7**, 1180–1190.
- Fan J, Urban M, Parker JE *et al.*, 2013. Characterization of the sterol 14 α -demethylases of *Fusarium graminearum* identifies a novel genus-specific CYP51 function. *New Phytologist* **198**, 821–835.
- Francis SA, 2006. Development of sugar beet. *Sugar beet*, 9–29.

- Gilmer D, Ratti C, Consortium IR, 2017. ICTV virus taxonomy profile: Benyviridae. *The Journal of general virology* **98**, 1571.
- Goodwin SB, Dunkle LD, Zismann VL, 2001. Phylogenetic analysis of *Cercospora* and *Mycosphaerella* based on the internal transcribed spacer region of ribosomal DNA. *Phytopathology* **91**, 648–658.
- Hao W, Li H, Hu M, Yang L, Rizwan-ul-Haq M, 2011. Integrated control of citrus green and blue mold and sour rot by *Bacillus amyloliquefaciens* in combination with tea saponin. *Postharvest Biology and Technology* **59**, 316–323.
- Harveson RM, Hein GL, Smith JA, Wilson RG, Yonts CD, 2002. An Integrated Approach to Cultivar Evaluation and Selection for Improving Sugar Beet Profitability: A Successful Case Study for the Central High Plains. *Plant disease* **86**, 192–204.
- Hawkins NJ, Bass C, Dixon A, Neve P, 2019. The evolutionary origins of pesticide resistance. *Biological Reviews* **94**, 135–155.
- Heick TM, Justesen AF, Jørgensen LN, 2017. Resistance of wheat pathogen *Zymoseptoria tritici* to DMI and QoI fungicides in the Nordic-Baltic region - a status. *European Journal of Plant Pathology* **149**, 669–682.
- Herr I, 1970. Disc-Plate Method for Selective Isolation of *Rhizoctonia* From Soil. In: *Phytopathology*. Amer Phytopathological Soc 3340 Pilot Knob Road, ST Paul, MN 55121, 1295.
- Herr LJ, 1996. Sugar Beet Diseases Incited by *Rhizoctonia* Spp. In: *Rhizoctonia species: taxonomy, molecular biology, ecology, pathology and disease control*. Springer, 341–349.
- Holtschulte B, 2000. *Cercospora beticola*—worldwide distribution and incidence. *Cercospora beticola*, 5–16.
- Hubbard RE, Haider MK, 2010. Hydrogen bonds in proteins: role and strength. *eLS*.
- Huf A, Rehfus A, Lorenz KH, Bryson R, Voegelé RT, Stammler G, 2018. Proposal for a new nomenclature for CYP 51 haplotypes in *Zymoseptoria tritici* and analysis of their distribution in Europe. *Plant Pathology* **67**, 1706–1712.
- Hughes AL, Todd BL, Espenshade PJ, 2005. SREBP pathway responds to sterols and functions as an oxygen sensor in fission yeast. *Cell* **120**, 831–842.
- Jacobsen BJ, Franc GD, 2009. *Cercospora* leaf spot. *Compendium of beet diseases and pests* **2**, 7–10.

- Kaiser U, Varrelmann M, 2009. Development of a field biotest using artificial inoculation to evaluate resistance and yield effects in sugar beet cultivars against *Cercospora beticola*. *European journal of plant pathology* **124**, 269–281.
- Karaoglanidis GS, Bardas G, 2006. Control of benzimidazole-and DMI-resistant strains of *Cercospora beticola* with strobilurin fungicides. *Plant disease* **90**, 419–424.
- Karaoglanidis GS, Ioannidis PM, Thanassoulopoulos CC, 2000. Reduced sensitivity of *Cercospora beticola* isolates to sterol-demethylation-inhibiting fungicides. *Plant Pathology* **49**, 567–572.
- Karaoglanidis GS, Karadimos DA, Ioannidis PM, Ioannidis PI, 2003. Sensitivity of *Cercospora beticola* populations to fenitrothion, benomyl and flutriafol in Greece. *Crop protection* **22**, 735–740.
- Kayamori M, Zakharycheva A, Saito H, Komatsu K, 2021. Resistance to demethylation inhibitors in *Cercospora beticola*, a pathogen of sugar beet in Japan, and development of unique cross-resistance patterns. *European Journal of Plant Pathology* **160**, 39–52.
- Kolaczowska A, Manente M, Kolaczowski M, Laba J, Ghislain M, Wawrzycka D, 2012. The regulatory inputs controlling pleiotropic drug resistance and hypoxic response in yeast converge at the promoter of the aminocholesterol resistance gene RTA1. *FEMS yeast research* **12**, 279–292.
- Krug JC, 2004. Moist chambers for the development of fungi. *Biodiversity of fungi. Academic Press, Burlington*, 589–593.
- Kumar R, Mazakova J, Ali A *et al.*, 2021. Characterization of the Molecular Mechanisms of Resistance against DMI Fungicides in *Cercospora beticola* Populations from the Czech Republic. *Journal of Fungi* **7**, 1062.
- Lepesheva GI, Waterman MR, 2007. Sterol 14 α -demethylase cytochrome P450 (CYP51), a P450 in all biological kingdoms. *Biochimica et biophysica acta (BBA)-General subjects* **1770**, 467–477.
- Liu TT, Lee RE, Barker KS *et al.*, 2005. Genome-wide expression profiling of the response to azole, polyene, echinocandin, and pyrimidine antifungal agents in *Candida albicans*. *Antimicrobial agents and chemotherapy* **49**, 2226–2236.
- Lugtenberg BJ, Caradus JR, Johnson LJ, 2016. Fungal endophytes for sustainable crop production. *FEMS microbiology ecology* **92**.

- Ma Z, Proffer TJ, Jacobs JL, Sundin GW, 2006. Overexpression of the 14 α -Demethylase Target Gene (CYP51) Mediates Fungicide Resistance in *Blumeriella jaapii*. *Applied and Environmental Microbiology* **72**, 2581–2585.
- MacPherson S, Akache B, Weber S, De Deken X, Raymond M, Turcotte B, 2005. *Candida albicans* zinc cluster protein Upc2p confers resistance to antifungal drugs and is an activator of ergosterol biosynthetic genes. *Antimicrobial agents and chemotherapy* **49**, 1745–1752.
- Mair WJ, Deng W, Mullins JGL *et al.*, 2016. Demethylase Inhibitor Fungicide Resistance in *Pyrenophora teres* f. sp. *teres* Associated with Target Site Modification and Inducible Overexpression of Cyp51. *Frontiers in Microbiology* **7**.
- Majumdar A, Yang X, Luo W, Chowdhury S, Chakraborty S, Ahuja R, 2020. High exothermic dissociation in van der Waals like hexagonal two dimensional nitrogen from first-principles molecular dynamics. *Applied Surface Science* **529**, 146552.
- Manente M, Ghislain M, 2009. The lipid-translocating exporter family and membrane phospholipid homeostasis in yeast. *FEMS Yeast Research* **9**, 673–687.
- Mazumdar A, Haddad Y, Milosavljevic V *et al.*, 2020. Peptide-Carbon Quantum Dots conjugate, Derived from Human Retinoic Acid Receptor Responder Protein 2, against Antibiotic-Resistant Gram Positive and Gram Negative Pathogenic Bacteria. *Nanomaterials* **10**, 325.
- McGrann GR, Grimmer MK, MUTASA-GÖTTGENS ES, Stevens M, 2009. Progress towards the understanding and control of sugar beet rhizomania disease. *Molecular plant pathology* **10**, 129–141.
- Mechelke W, 2000. Züchtungs-und Sortenstrategien zur Resistenz bei Zuckerrüben gegenüber *Cercospora beticola*. *Zuckerindustrie* **125**, 688–692.
- Meyer V, Damveld RA, Arentshorst M, Stahl U, van den Hondel CAMJJ, Ram AFJ, 2007. Survival in the Presence of Antifungals: GENOME-WIDE EXPRESSION PROFILING OF *ASPERGILLUS NIGER* IN RESPONSE TO SUBLETHAL CONCENTRATIONS OF CASPOFUNGIN AND FENPROPIMORPH*. *Journal of Biological Chemistry* **282**, 32935–32948.
- Miller J, Rekoske M, Quinn A, 1994. Genetic resistance, fungicide protection and variety approval politics for controlling yield losses from *Cercospora* leaf spot infection. *J. Sugar Beet Res* **31**, 7–12.

- Muellender MM, Mahlein A-K, Stammer G, Varrelmann M, 2021. Evidence for the association of target-site resistance in *cyp51* with reduced DMI sensitivity in European *Cercospora beticola* field isolates. *Pest Management Science* **77**, 1765–1774.
- Mullins JGL, Parker JE, Cools HJ *et al.*, 2011. Molecular Modelling of the Emergence of Azole Resistance in *Mycosphaerella graminicola*. *PLOS ONE* **6**, e20973.
- Nikou D, Malandrakis A, Konstantakaki M, Vontas J, Markoglou A, Ziogas B, 2009. Molecular characterization and detection of overexpressed C-14 alpha-demethylase-based DMI resistance in *Cercospora beticola* field isolates. *Pesticide Biochemistry and Physiology* **95**, 18–27.
- Ossenkop A, Ladewig E, Manthey R, 2002. Leistung von cercosporaresistenten Sorten: Konsequenzen für Prüfsysteme und Anbauberatung. *Zuckerindustrie* **127**, 867–871.
- Papavizas GC, 1974. *Aphanomyces* species and their root diseases in pea and sugarbeet: a review.
- Parker JE, Warrilow AGS, Price CL, Mullins JGL, Kelly DE, Kelly SL, 2014. Resistance to antifungals that target CYP51. *Journal of Chemical Biology* **7**, 143–161.
- Piszczyk J, 2004. RESISTANCE OF SELECTED STRAINS OF *CERCOSPORA BETICOLA*. *Postępy w ochronie roślin* **44**, 1031.
- Protchenko O, Shakoury-Elizeh M, Keane P, Storey J, Androphy R, Philpott CC, 2008. Role of PUG1 in inducible porphyrin and heme transport in *Saccharomyces cerevisiae*. *Eukaryotic cell* **7**, 859–871.
- Rangel LI, Spanner RE, Ebert MK *et al.*, 2020a. *Cercospora beticola*: The intoxicating lifestyle of the leaf spot pathogen of sugar beet. *Molecular Plant Pathology* **21**, 1020–1041.
- Rangel LI, Spanner RE, Ebert MK *et al.*, 2020b. *Cercospora beticola*: The intoxicating lifestyle of the leaf spot pathogen of sugar beet. *Molecular Plant Pathology* **21**, 1020–1041.
- Řezbová H, Belová A, Škubna O, 2013. Sugar beet production in the European Union and their future trends. *Agris on-line Papers in Economics and Informatics* **5**, 165–178.
- Richardson K, 2010. Traditional Breeding in Sugar Beet. *Sugar Tech* **12**, 181–186.
- Robbertse B, van der Rijst M, van Aarde IMR, Lennox C, Crous PW, 2001. DMI sensitivity and cross-resistance patterns of *Rhynchosporium secalis* isolates from South Africa. *Crop Protection* **20**, 97–102.

- Robinson MD, McCarthy DJ, Smyth GK, 2010. edgeR: a Bioconductor package for differential expression analysis of digital gene expression data. *bioinformatics* **26**, 139–140.
- Rosenzweig N, Hanson LE, Mambetova S *et al.*, 2019. Fungicide sensitivity monitoring of *Alternaria* spp. causing leaf spot of sugarbeet (*Beta vulgaris*) in the Upper Great Lakes. *Plant disease* **103**, 2263–2270.
- Rossi V, 1995. Effect of host resistance in decreasing infection rate of *Cercospora* leaf spot epidemics on sugarbeet. *Phytopathologia Mediterranea*, 149–156.
- Rossi V, Battilani P, Chiusa G, Giosue S, Languasco L, Racca P, 1999. Components of rate-reducing resistance to *Cercospora* leaf spot in sugar beet: incubation length, infection efficiency, lesion size. *Journal of Plant Pathology*, 25–35.
- Rossi V, Battilani P, Chiusa G, Giosue S, Languasco L, Racca P, 2000. Components of rate-reducing resistance to *Cercospora* leaf spot in sugar beet: conidiation length, spore yield. *Journal of Plant Pathology*, 125–131.
- Secor GA, Rivera VV, Khan MFR, Gudmestad NC, 2010. Monitoring Fungicide Sensitivity of *Cercospora beticola* of Sugar Beet for Disease Management Decisions. *Plant Disease* **94**, 1272–1282.
- Sen MK, Hamouzová K, Mikulka J *et al.*, 2021. Enhanced metabolism and target gene overexpression confer resistance against acetolactate synthase-inhibiting herbicides in *Bromus sterilis*. *Pest Management Science* **77**, 2122–2128.
- Shane WW, Teng PS, 1992. Impact of *Cercospora* leaf spot on root weight, sugar yield, and purity of *Beta vulgaris*. *Plant disease* **76**, 812–820.
- Shrestha S, Neubauer J, Spanner R *et al.*, 2020. Rapid detection of *Cercospora beticola* in sugar beet and mutations associated with fungicide resistance using LAMP or probe-based qPCR. *Plant disease* **104**, 1654–1661.
- Sierotzki H, Scalliet G, 2013. A review of current knowledge of resistance aspects for the next-generation succinate dehydrogenase inhibitor fungicides. *Phytopathology* **103**, 880–887.
- Soustre I, Letourneux Y, Karst F, 1996. Characterization of the *Saccharomyces cerevisiae* RTA1 gene involved in 7-aminocholesterol resistance. *Current genetics* **30**, 121–125.

- Spanner R, Taliadoros D, Richards J *et al.*, 2021. Genome-wide association and selective sweep studies reveal the complex genetic architecture of DMI fungicide resistance in *Cercospora beticola*. *Genome biology and evolution* **13**, evab209.
- Steinkamp MP, Martin SS, Hoefert LL, Ruppel EG, 1979. Ultrastructure of lesions produced by *Cercospora beticola* in leaves of *Beta vulgaris*. *Physiological Plant Pathology* **15**, 13–26.
- Stevanato P, Broccanello C, Biscarini F *et al.*, 2014. High-throughput RAD-SNP genotyping for characterization of sugar beet genotypes. *Plant molecular biology reporter* **32**, 691–696.
- Tamada T, Kondo H, 2013. Biological and genetic diversity of plasmodiophorid-transmitted viruses and their vectors. *Journal of general plant pathology* **79**, 307–320.
- Trkulja NR, Milosavljević AG, Mitrović MS *et al.*, 2017. Molecular and experimental evidence of multi-resistance of *Cercospora beticola* field populations to MBC, DMI and QoI fungicides. *European Journal of Plant Pathology* **149**, 895–910.
- Tyndall JD, Sabherwal M, Sagatova AA *et al.*, 2016. Structural and functional elucidation of yeast lanosterol 14 α -demethylase in complex with agrochemical antifungals. *PloS one* **11**, e0167485.
- Vaghefi N, Kikkert JR, Bolton MD, Hanson LE, Secor GA, Pethybridge SJ, 2017. De novo genome assembly of *Cercospora beticola* for microsatellite marker development and validation. *Fungal Ecology* **26**, 125–134.
- Van Swaaij A, Heijbroek W, Basting JL, 2001. Testing and improving seed vigour in sugar beet. In: *64th Congress, Institut International de Recherches Betteravières, Bruges, Belgium, 26-27 June 2001*. Institut International de Recherches Betteravieres, 237–246.
- Wei L, Chen W, Zhao W *et al.*, 2020. Mutations and Overexpression of CYP51 Associated with DMI-Resistance in *Colletotrichum gloeosporioides* from Chili. *Plant disease* **104**, 668–676.
- Weiland JJ, Halloin JM, 2001. Benzimidazole resistance in *Cercospora beticola* sampled from sugarbeet fields in Michigan, USA. *Canadian Journal of Plant Pathology* **23**, 78–82.
- Weiland J, Koch G, 2004. Sugarbeet leaf spot disease (*Cercospora beticola* Sacc.). *Molecular plant pathology* **5**, 157–166.
- Windels CE, 2000. Aphanomyces root rot on sugar beet. *Plant Health Progress* **1**, 8.

- Windels CE, Brantner JR, Sims AL, Bradley CA, 2007. Long-term effects of a single application of spent lime on sugar beet, *Aphanomyces* root rot, rotation crops, and antagonistic microorganisms. *Sugar Beet Research and Extension Reports* **38**, 251–262.
- Wolf PFJ, Kraft R, Verreet JA, 1998. Characteristics of damage caused by *Cercospora beticola* (Sacc) in sugar beet as a base of yield loss forecast. *Zeitschrift für Pflanzenkrankheiten und Pflanzenschutz* **105**, 462–474.
- Wolf PFJ, Verreet JA, 2002. An integrated pest management system in Germany for the control of fungal leaf diseases in sugar beet: The IPM sugar beet model. *Plant disease* **86**, 336–344.
- Wolf PFJ, Verreet JA, 2005. Factors affecting the onset of *Cercospora* leaf spot epidemics in sugar beet and establishment of disease-monitoring thresholds. *Phytopathology* **95**, 269–274.
- Wolf PF, Verreet J-A, 2009. Empirical-deterministic prediction of disease and losses caused by *Cercospora* leaf spots in sugar beets. *Journal für Kulturpflanzen-Journal of Cultivated Plants* **61**, 168.
- Zhang J, Li L, Lv Q, Yan L, Wang Y, Jiang Y, 2019. The fungal CYP51s: Their functions, structures, related drug resistance, and inhibitors. *Frontiers in microbiology* **10**, 691.
- Zhang Y, Mao C-X, Zhai X-Y, Jamieson PA, Zhang C-Q, 2021. Mutation in *cyp51b* and overexpression of *cyp51a* and *cyp51b* confer multiple resistant to DMIs fungicide prochloraz in *Fusarium fujikuroi*. *Pest Management Science* **77**, 824–833.
- Zhou Y, Chen L, Hu J *et al.*, 2015. Resistance Mechanisms and Molecular Docking Studies of Four Novel QoI Fungicides in *Peronospora litchii*. *Scientific Reports* **5**, 17466.